Universidade de Lisboa

Faculdade de Farmácia

Investigation of MAT2A dependency in Acute Myeloid Leukaemia

A preliminary study in Acute Myeloid Leukaemia cell lines

Rita Romano Ferreira Betencourt Adão

Mestrado Integrado em Ciências Farmacêuticas

2017

Universidade de Lisboa

Faculdade de Farmácia

Investigation of MAT2A dependency in Acute Myeloid Leukaemia

A preliminary study in Acute Myeloid Leukaemia cell lines

Rita Romano Ferreira Betencourt Adão

Monografia de Mestrado Integrado em Ciências Farmacêuticas apresentada à Universidade de Lisboa através da Faculdade de Farmácia

Orientador: Prof. Dr. Susana Solá

2017

Final Report

Erasmus programme

University of Cambridge Department of Haematology

UNIVERSITY OF CAMBRIDGE

Rita Romano Ferreira Betencourt Adão

Supervisor (Univ. of Cambridge): Intermediate Fellow

Cristina Pina

2017

The work presented in this thesis was developed in the Department of Haematology of the University of Cambridge, Cambridge Biomedical Campus, Cambridge, United Kingdom. The work was integrated in Erasmus+ Programme and was conducted under the supervision of Dr. Cristina Pina.

Acknowledgements

Foremost, I would like to start by expressing my sincere gratitude to Doutora Cristina Pina for receiving me and accept me in her laboratory group. Thank to her I experienced a new vision of the research field, I could achieve a new degree of knowledge, and learn new and different subjects apart from my pharmaceutical background. She offered me a once-in-a-lifetime opportunity and I will always be thankful for her time and her careful attention to detail, for the instructions she gave me throughout this project, for believing in my work and proposing me new challenges.

Also, a very special gratitude goes out to professor Susana Solá. First for her acceptance, support and guidance through the writing of this thesis. And I also take this opportunity to thank for her assistance during my academic and professional education and throughout other projects. For her time, experience and knowledge in everything.

To all Cambridge laboratory team, but with a special gratitude to Filipa Domingues. It was thanks to her sympathy, her big transmission of knowledge and to her big dedication in teaching me that I could thrive and learn every day a little more. You were certainly the best mentor I could have. Nevertheless, I am also grateful to have met Selinde. Thanks to her support, kindness, craziness and most important her sharing experience. Thank you for all the good moments inside and outside the laboratory. All people from the lab were always very dedicated, helpful and friendship. Thank you all.

I cannot fail to thank Marco, Marloes, Maria and Teresa. This journey would not have been possible without their support in so different ways. Thank them for all the support they gave me. Thanks for sharing moments and stories through our journey. I wish them a brilliant future, full of success, health and happiness!

Likewise, an enormous thank to my friends, and they know, for our meetings, well-wishes, phone and skype calls, visits, advices, and being there whenever I needed.

Most importantly, none of this would be possible without the love and patience of my family, specially my mum, dad and my sister Mariana. Thank you for providing me this unique experience, for all your sacrifices, for giving me strength and encourage. I am what I am thanks to you and with your support I could reach this step. I am also

grateful to my other family members who, probably without knowing, have supported me along the way. A special thanks to André for all patience, unfailing support, care and encouragement throughout my life and in particularly through this laborious step.

I could not conclude without thank to sci-hub.bz.

List of abbreviations

5-mTHF	5-methyltetrahydrafolate
AML	Acute myeloid leukemia
AmpR	Ampicillin resistance
BCL2	B-cell lymphoma 2
BFP	Blue fluorescent protein
C/EBPα	CCAAT/enhancer binding protein-α
CBFβ	Core-binding factor-β
CBL	Cbl proto-oncogene
CDS	Coding sequence
CIMR	Cambridge Institute for Medical Research
CMV	Cytomegalovirus
CO_2	Chemical formula for Carbon dioxide
CRISPR	Clustered regularly interspaced short palindromic repeats
DEPC	Diethylpyrocarbonate
DMEM	Dulbecco's modified eagle's medium
DNA	Deoxyribonucleic acid
DNMT3A	DNA (cytosine-5)-methyltransferase 3A
FAB	French–american–british
FACS	Fluorescence-activated cell sorting
FBS	Fetal bovine serum
FLT3	Receptor-type tyrosine-protein kinase
Fw	Forward
GFP	Green fluorescent protein
GTP	Guanosine-5'-triphosphate
H3K4	Lysine 4 in histone H3
hCys	Homocysteine
HMTs	Histone methyltransferases
ITD	Internal tandem duplications
KD	Knockdown
KO	Knockout

LB	Lysogeny broth or also commonly, Luria broth or Luria-Bertani medium
LMA	AML in portuguese: leucemia mieloide aguda
MAT	Methionine adenosyltransferase
MAT2A	Methionine adenosyltransferase2a
MET	Methionine
MLL	Mixed lineage leukaemia
MM	MasterMix
MS	Methionine synthase
NEB	New england biolabs
Nm	Nanometers
NPM1	Nucleophosmin
PCR	Polymerase chain reaction
PGK	Phosphoglycerate kinase
pLL3.7	Lentilox 3.7
PML	Promyelocytic leukaemi
PU.1	Transcription factor encoded by SPI1
RARα	Retinoic acid receptor-α
RAS	Small gtpases
RISC	RNA-induced silencing complex
RNA	Ribonucleic acid
RNAi	RNA interference
RPM	Revolutions per minute
RT-qPCR	Quantitative reverse transcription polymerase chain reaction
RUNX1	Runt-related transcription factor 1
RUNX1T1	Runx1 translocation partner 1
Rv	Reverse
SAH	S-adenosylhomocysteine
SAM	S-adenosylmethionine
sgRNA	Single guide RNA
shRNA	Short hairpin rnas
TAE	Tris-acetate-EDTA

List of figures

Figure 1 - CRISPR-Cas9 target recognition. The sgRNA (in green) hybridizes with the strand opposite the PAM site (in red), where the transcript RNA (in yellow) is important to binding the Cas9 protein. After, the Cas9 nuclease cuts the DNA, giving rise to a site-specific double strand DNA (dsDNA) break. Ref: http://www.genecopoeia.com/product/genome-editing-tools/genome-editing/ 7

Figure 2 – shRNAs mechanism. Lentiviral delivery and machinery of RNA interference (iRNA) in mammalian cells until the last step of translational suppression or mRNA cleavage. GAG indicates glycosaminoglycans; VSVg, component of vector envelope. Ref: Dan Cojocari, Department of Medical Biophysics, University of Toronto, 2010. 8

Figure 3 - One-carbon metabolism and histone methylation. Methionine adenosyltransferase (MAT) uses methionine (MET) to form S-Adenosylmethionine (SAM) and histone methyltransferases (HMTs) utilize SAM to donate a methyl group to their histone substrates. While histone demethylases (HDMs) remove the methyl group from histones now methiylated, the resulted S-adenosylhomocysteine (SAH) is converted to homocysteine (hCys) via S-adenosylhomocysteine hydrolase (SAHH). In turn, hCys can be remethylated to regenerate MET by donation of a methyl group from 5-methyltetrahydrafolate (5-mTHF) via methionine synthase (MS) or from betaine via betaine–homocysteine S-methyltransferase (BHMT). 9

Figure 4 - Methionine cycle and trans-sulfuration pathway. Glutathione synthesis starts with the conversion of homocysteine into cystathionine, which is dependent on the presence of both serine and cystathionine β-synthase. Cystathionine origins cysteine by cystathionase and with a loss of a- ketobutyrate. In turn, cysteine origins γ-glutamylcysteine with the use of glutamine and γ-glutamylcysteine ligase, and finally, depending on glycine and glutathione synthetase, glutathione is formed. 10

Figure 5 – Dimeric composition of MAT enzyme. MAT1A and MAT2A encode two MAT catalytic subunits, α1 and α2, correspondingly. The α1 subunit organizes into dimers (MATIII) or tetramers (MATI). The α2 subunit is found in the MATII isoform. A third gene MAT2B, encodes a regulatory subunit β, that regulates the activity of MATII. 11

Figure 6 - Schematic representation of results of the Tzelepis et al CRISPR/Cas9 drop-out screen for MAT2A, evidencing the need of MAT2A for maintenance of AML cell lines. Significant p-values for gene drop-out represented in colour at different levels of FDR (yellow<20%; gold<10%; orange<5%; brown<1%); grey, not significant. 12

Figure 7 - A) Design of pKLV2 vector. Expresses gRNA under the pol III U6 promoter. The plasmid contains a PGK promoter cassette to monitor expression of gRNAs. The bacterial plasmid is resistant to ampicillin, since the AmpR cassette is present. Restriction enzymes BbsI cut two sticky ends, which are responsible to attach the designed gRNAs, complementary to the restriction ends. B) Excerpt of pKLV2 plasmid sequence where we can see the sequencing cut recognized by BbsI restricted enzymes, creating two sticky ends that bind guideRNAs for Mat2a and MAT2A genes. 16

Figure 8 - A) Design of pLL3.7 vector. Expresses shRNA under the pol III U6 promoter. The plasmid contains a CMV promoter cassette to monitor expression of shRNA. The bacterial plasmid is resistant to ampicillin, since the AmpR cassette is present. Restriction enzymes HpaI cuts the 3' cloning site bluntly, where XhoI leaves a sticky end when cutting the 5' cloning site, open for binding of the designed oligos to complement the restriction ends. B) Exert of Pll3.7 plasmid sequence where we can see the cut sequencing recognized by restricted enzymes..... 17

Figure 9 - Example of sort plots. A) Gating strategy for Gallios flow cytometry. First histogram shows a gate to select living cells, through forward scatter-FS and side scatter-SS. FS detects cell size and SS determines the granularity and complexity of the cell. To exclude doublets, a second gate was established contemplating only living cells (SS Width vs. SS Area). Then, singlets were gated on BFP positivity. The third histogram shows the negative control, with uninfected cells, in which we based to determine the negative population for BFP positive. B) Example of a BFP positive population, that shows the percentage of transduced cells. These graphs resulted from MOLM13 cells. 25

Figure 10 - Example of FACS analysis and sort of living cells transduced with BFP. A) Gating selection using a negative control unstained. i. shows the gate for live cells (SSC-A vs. FSC-A). ii. From these a second gate was drawn to separate singlets from doublets (FSC-W vs. FSC-A). iii. Singlets were gated for BFP positivity. B) Example of a BFP+ population being sorted. C) Scheme that shows all different cells in the culture. All histograms correspond to MOLM13 cells; A- MOLM13 CTRL, B- MOLM13 transduced with gMAT2A. 26

Figure 11 – Excerpt of pKLV2 plasmid sequence showing BbsI cloning sites either side of the guide RNA scaffold. BbsI digestion generates 2 unique cohesive ends used for insertion of individual gRNAs..... 29

Figure 12 – Excerpt of pKLV2 plasmid sequence with the 2th guide designed for human MAT2A gene (see sequence in Materials and Methods) incorporated. Guide RNAs are designed as two complementary oligonucleotides with unique ends that complement the unique cohesive ends generated through BbsI digestion of pKLV2. 29

Figure 13 – Example of a BbsI digestion gel. This gel shows digestion bands of samples with gRNA DNA (non-digested, 1-5 and digested, 1'-5') and the positive and negative controls, represented as non-digested (ND) and digested (D). 30

Figure 14 - A) Live cells /mL and B) % of Cell Death of one performed experiment (n=1). In a general way, Oci-AML3-EV sample proliferates and increases the cell culture. On the other side, MAT2A sample is marked by cell death, with no room to increase cell culture, so that it does not expand like EV sample does. 31

Figure 15 - A) Live cells /mL and B) % of Cell Death of one performed experiment (n=1). Here, there is no expansion in cell culture of MAT2A sample once the culture growth does not increase and % of cell death is decreasing with the concentration decrement. The opposite is verified in EV sample, inasmuch cell culture is expanding while the % of cell death is decreasing. 31

Figure 16 - A) Live cells /mL and B) % of Cell Death of one performed experiment (n=1). EV sample has a higher culture expansion comparing with MAT2A sample, which is marked by a 50% of cell death in the last days of the followed experiment. 32

Figure 17 - Example of a matching sequence of a positive clone with a mouse forward guide (Fw: CACCGAGAAACTGTTGCTAAAAC), done by Source BioScience UK Limited. Of note, it only need one wrong base to be a non-recombinant sequence. 33

Figure 18 – A) Live cells /mL and B) % of Cell Death of one performed experiment (n=1). While EV sample recovers and we see a huge proliferation, the same does not happen with the Mat2a sample, in which the % of cell death surpassed the proliferation and so Mat2a sample ends up dying. 34

Figure 19 - A) Live cells /mL and B) % of Cell Death of a performed triplicate experiment (n=3). 35

Figure 20 - Digestion gels. A) showing the negative control non-digested and both wells with digested product. B) showing the cut out of plasmid DNA to former use gel extraction kit. 36

Figure 21 – A) 1 Kb Plus DNA ladder for a 2% agarose gel with quantity of base pairs per bar represented. B) Gel of DNA multiplied by PCR screen, run on a 2% agarose gel. First loading well contained the 1 Kb plus DNA ladder, followed by 12 samples. Three controls followed next: negative and positive controls to be able to detect positive clones, and a blanc control to check for contamination. Positive samples, which are the ones with the shRNA inserted, are represented in the same line of the positive control, a little higher than the negative samples. These last ones, as we can see clearly in the samples 6 and 8, don't have the shRNA inserted, since the used primers cannot amplify the inserted shRNA region. Red arrows indicate positive

clones, which were sent for sequencing. This gel shows bands of shMAT2A_1 (1-8) and shMAT2A_2 (9-12) DNA. 36

Figure 22 - BamHI digestion for screen for positive clones, run on a 0.8% agarose gel. First loading well, in both gels, contained the 1 Kb plus DNA ladder, followed by the samples, in which the numbers (1) represent undigested plasmid and the numbers followed by the sign ‘ (1’), represent the digested vector. Positive and negative controls run in the gel 2, in the last 4 wells. Positive clones had the same appearance as the positive control. When digested, the positive clones appear as linearized plasmid, while the non-digested appears as a circular plasmid. Red arrows indicate positive clones, which were sent for sequencing. This gel shows the difference of digested (1-12) and non-digested (1’-12’) samples of shMAT2A_2. 37

Figure 23 - Example of matching sequences of a positive clone with shMAT2A, Fw and Rv (shMAT2A-2 Fw:TGTTCAGGTCTCTTATGCTATTGGGATCCAATAGCATAAGAGACCTGAACTTTTTTC), done by Source BioScience UK Limited. 38

Figure 24 - MAT2A expression relative to ACTB and GAPDH controls, individually. Relative to both controls, the expression level of MAT2A gene dropped to 27 and 25%, respectively. Standard Deviation error bars indicate that KD relative to ACTB has an error of 2% and relative to GAPDH the error can go up until 7%. 39

Figure 25 – A) Live cells /mL and B) % of Cell Death of a performed duplicate experiment (n=2). In general, LLX CTRL samples increase proliferation, reducing cell death. Meanwhile, in shMAT2A cells, we do not observe cell culture expansion, and cell death path is not regular, decreasing day-by-day in one sample (shMAT2A-1) and decreasing first until day 3 but ending up dying in the last day in the other sample (shMAT2A-2), with a 100% of cell death. 40

Figure 26 – CDS sequence of MAT2A gene. Guides location are represented in orange rectangles. Primer sets are highlighted with a purple arrow and the tip and toes of the exons are also represented with different colour arrows for each exon. Figure was designed with SnapGene Viewer 3.3.3. Gene mRNA sequence was taken out from (“MAT2A methionine adenosyltransferase 2A [Homo sapiens (human)],” n.d.)..... 42

Figure 27 – A) Dissociation curve of the qPCR test with annealing temperature set at 65,25 °C showing high peak at ± 84,5 ºC of four populations in a n=3 experiment: MOLM13-EV, MOLM13-MAT2A, Oci-AML3-EV and Oci-AML3-MAT2A, which correspond to MAT2A primer set that span the exons 1 and 2. 43

Figure 28 – MAT2A expression relative to ACTB and GAPDH controls, individually, regarding both MAT2A primer sets. Red columns correspond to RT-qPCR using MAT2A

primers spanning exons 1 and 2 of gMAT2A samples, while green columns are related with MAT2A primers that span exons 6 and 7. Considering all conditions, no considerable loss of MAT2A gene expression is observed. A) Related with MOLM13 cell line. B) Related with Oci-AML3 cell line. 43

List of tables

Table 1 - FAB classification of Acute Myeloid Leukemia, highlighting some morphological characteristics as well as the prevalence of each type in adult patients with AML. *Prevalence in adult AML patients. ..... **Erro! Marcador não definido.**

Table 2 - Examples of transcription factor mutations in patients with AML, regarding the chromosomal location, the frequency that occur in AML patients and the most common FAB subtype associated. AML, acute myeloid leukaemia; CBFβ, core-binding factor-β; C/EBPα, CCAAT/enhancer binding protein-α; FAB, French–American–British; MLL, mixed lineage leukaemia; H3K4, lysine 4 in histone H3;MYH11, myosin heavy chain 11; PML, promyelocytic leukaemia; PU.1, transcription factor encoded by SPI1; RARα, retinoic acid receptor-α; RUNX1, runt-related transcription factor 1. ..... **Erro! Marcador não definido.**

Table 3 - Examples of gene mutations in patients with AML, regarding the chromosomal location, the frequency that occur in AML patients. AML, acute myeloid leukaemia; C/EBPα, CCAAT/enhancer binding protein-α; MLL, mixed lineage leukaemia; NPM1, Nucleo-phosmin 1; FLT3, fms like tyrosine kinase 3; ITD, Internal Tandem Duplication; BAX, BCL2-associated X protein; DNMT3A, DNA (cytosine-5)-methyltransferase 3A. **Erro! Marcador não definido.**

Table 4 - Sequences (5'-3') of forward (Fw) and reverse (Rv) guides for human MAT2A gene. 18

Table 5 - Sequences (5'-3') of forward (Fw) and reverse (Rv) guides for human MAT2A gene. ..... **Erro! Marcador não definido.**

Table of Contents

ACKNOWLEDGEMENTS VII
LIST OF ABBREVIATIONS IX
LIST OF FIGURES XI
LIST OF TABLES XVI
TABLE OF CONTENTS XVII
ABSTRACT XIX
RESUMO XX
1. INTRODUCTION 1
1.1. ACUTE MYELOID LEUKEMIA 1
1.2. GENE EDITING 6
1.3. ACUTE MYELOID LEUKEMIA AND MAT2A 8
2. OBJECTIVES 12
3. MATERIALS AND METHODS 13
3.1. CELL LINES 13
3.1.1. MOUSE CELL LINES 13
3.1.2. HUMAN CELL LINES 13
3.2. CELL CULTURE 14
3.3. PLASMID CONSTRUCTION 15
3.3.1. PKLV2 VECTOR FOR GUIDERNA. 15
3.3.2. LENTILOX 3.7 VECTOR FOR SHORT HAIRPIN RNA (SHRNA). 16
3.4. GRNA AND SHRNA DESIGN 17
3.4.1. GRNAS 17
3.4.2. SHRNAS 18
3.5. CLONING GRNA AND SHRNAS: ANNEALING, LIGATION AND TRANSFORMATION 19
3.5.1. GLYCEROL STOCKS 20
3.6. SCREEN FOR POSITIVE CLONES 21
3.6.1. GRNA CLONES – BBSI DIGESTION 21
3.6.2. SHRNA CLONES – PCR SCREENING AND BAMHI DIGESTION 21
3.7. ISOLATION OF BACTERIAL PLASMID DNA 22
3.7.1. GRNA CLONES 22
3.7.2. SHRNA CLONES 23
3.7.3. DNA QUANTIFICATION 23
3.8. LENTIVIRUS PRODUCTION AND TRANSDUCTION 23
3.8.1. VIRAL TRANSDUCTION WITH GUIDE RNAS 24
3.8.2. VIRAL TRANSDUCTION WITH SHORT HAIRPIN RNAS FOR MAT2A GENE 24
3.9. FACS AND FACS-SORTING 25
3.10. ANALYSIS OF CELL GROWTH 27
3.11. RNA ISOLATION, PRIMER DESIGN AND RT-QPCR 27
4. RESULTS 29
4.1. MAT2A KNOCKOUT ABROGATES PROLIFERATION OF HUMAN AML CELL LINES 29
4.2. MAT2A KNOCKOUT ABROGATES PROLIFERATION OF TRANSFORMED PRIMARY MOUSE BONE MARROW CELL LINES 33
4.3. FUNCTIONAL VALIDATION OF CRISPR SCREEN 36
4.3.1. VALIDATION OF KNOCKDOWN 38

4.4. CONFIRMING DIRECT VALIDATION OF CRISPR SCREEN 41
5. CONCLUSIONS AND FUTURE PERSPECTIVES 45
6. REFERENCES 48
7. ANNEXES 54

Abstract

Acute Myeloid Leukemia (AML) is a disease of dismal prognosis, with a 5-year survival of under 40% that has remained unmodified for the last 3 decades. Sequencing analyses of patient samples have identified recurrent mutations and highlighted associated common disease mechanisms, which have putative therapeutic value. Additionally, loss-of-function genetic or expression knockdown screens can be used to identify individual factors required for disease maintenance that may not be targeted by mutation. A recent drop-out screen based on Clustered Regularly Interspaced Short Palindromic Repeats with the Cas9 endonuclease technology (CRISPR/Cas9) identified *MAT2A* (methionine adenosyltransferase2A) as a susceptibility gene in at least some forms of AML.

In the work reported in this thesis, I aimed to validate the results of the screen by confirming dependency of cultured AML cells on *MAT2A* expression. I selected AML cell lines representing distinct common subtypes of human leukaemia, and evaluated the effects of knocking-out *MAT2A* through CRISPR/Cas9 gene editing technology. As a complementary strategy, I developed and validated RNA interference (RNAi) tools for *MAT2A* expression knockdown, which are also amenable for testing in AML patient samples. I observed that *MAT2A* loss resulted in reduced proliferation and survival of cultured AML cells. These results are currently being pursued mechanistically with a view to establishing novel therapeutic strategies in AML.

Resumo

A Leucemia mieloide aguda (LMA) é uma doença com um prognóstico bastante reservado, na qual menos de 40% dos doentes sobrevivem até 5 anos após diagnóstico da doença, sendo que esta percentagem permaneceu inalterada desde as últimas 3 décadas. As análises de sequenciação de amostras de pacientes identificaram mutações recorrentes e destacaram mecanismos associados, que têm valor terapêutico putativo. Além disso, fazer um *screen* para avaliar perdas de função genética ou mesmo *knockdown* de expressão de genes, pode ser útil na medida em que certos fatores individuais podem ser necessários para a manutenção da doença sem que estes sejam alvo de mutação. Um recente *drop-out screen*, que tem como base ir avaliando as consequências da perda individual de todos os fatores, baseada na tecnologia CRISPR, que consiste em pequenas porções do DNA bacteriano compostas por repetições de nucleotídeos, associada à endonuclease Cas9 (CRISPR/Cas9) identificaram o gene *MAT2A* (metionina adenosiltransferase2A) como um gene susceptível em pelo menos algumas formas de LMA.

No trabalho exposto nesta tese, pretendi validar os resultados desse *screen*, confirmando a dependência das células com LMA cultivadas sobre a expressão de *MAT2A*. Selecionei linhas celulares com LMA que representavam subtipos comuns distintos de leucemia humana e avaliei os efeitos do *knockout* de *MAT2A* através da tecnologia de edição de genes CRISPR / Cas9. Como uma estratégia complementar, desenvolvi e legitimei ferramentas de RNA interferência (RNAi) para o *knockdown* de expressão de *MAT2A*, que também pode ser testado em amostras de pacientes com LMA. Observei que a perda de *MAT2A* resultou numa diminuição da proliferação e da sobrevivência nas células cultivadas com LMA. Estes resultados estão atualmente a ser seguidos mecanicamente com vista a estabelecer novas estratégias terapêuticas em LMA.

1. Introduction

1.1. Acute myeloid leukemia

Acute Myeloid Leukemia (AML) is a clonal hematopoietic disorder of undifferentiated myeloid precursors (blasts), characterized by abnormal expansion of immature white blood cells in the bone marrow, with accompanying impairment of normal hematopoiesis (1). Prognosis is dependent upon several factors, including subtype of AML, age and other chronic medical conditions. It is estimated to comprise around 34% of all cases of leukaemia in 2017 (2).

Leukemia is the name given to the white blood cells cancer and it is divided into 4 specific types, particularly with a myeloid or lymphocytic origin and an acute or chronic development. “Acute” implies fast disease progression if not treated and “Myeloid” refers to the type of cell this leukemia starts from. Conventional treatments of chemotherapy or even hematopoietic stem cell transplant have not changed for decades, so that it is urgent to find alternative ways to overcome the disease.

AML is clinically and molecularly heterogeneous (3). One system commonly used for AML classification is the French-American-British (FAB) classification. It divides the disease into subtypes, M0 through M7, based on the type of cell from which the leukemia develops and how mature the cells are (Table 1).

*Table 1 - FAB classification of Acute Myeloid Leukemia, highlighting some morphological characteristics as well as the prevalence of each type in adult patients with AML. *Prevalence in adult AML patients. Ref: Hoffman, 2010* (4)*; Acute Myeloid Leukemia Staging, Internet, accessed 12-10-2017* (5).

FAB classification		**Characteristics**	**Prevalence***
M0	Undefined acute myeloblastic leukemia.	Large and agranular blasts	5%
M1	Undifferentiated acute myeloblastic leukemia	Blast cells, agranular and granular types	15%

M2	Acute myeloblastic leukemia with minimal maturation	Sum of agranular and granular blasts	25%
M3	Acute promyelocytic leukemia (APL)	Abnormal promyelocytes with heavy granulation	10%
M4	Acute myelomonocytic leukemia	Sum of myeloblasts, promyelocytes, myelocytes and later granulocytes around 80%	20%
M4 eos	Acute myelomonocytic leukemia with eosinophilia	Abnormal eosinophils	5%
M5	Acute monocytic macrophage leukemia	Monoblasts, promonocytes, monocytes	10%
M6	Acute erythroid leukemia	Erythroid components exceed 50% of all nucleated cells.	5%
M7	Acute megakaryoblastic leukemia	More than 30% of nucleated cells are blasts	5%

Each particular type of AML, according to FAB classification, is characterized by a high degree of heterogeneity in what concerns chromosomal abnormalities and gene mutations, which may coexist together in leukemic cells (6).

Non-random chromosomal abnormalities, such as translocations, that result in functional gene arrangements, and production of oncogenic fusion proteins, have been found in more than 60% of patients with AML. Amongst these, I highlight the translocations between chromosomes 8 and 21 (t(8;21)), resulting in the RUNX1-RUNX1T1 fusion protein; between chromosomes 15 and 17 (t(15;17)), with synthesis of PML-RARα; and multiple rearrangements of chromosome 11q23 resulting in fusion proteins involving Mixed Lineage Leukemia (MLL) gene.

Table 2 shows the most frequent translocations with the respective chromosomal location, resulting onco-fusion proteins, and their effect on AML cells. In general, translocations are associated with transcriptional re-programming (7). For example, RUNX1– RUNX1T1 down-regulates expression or activity of PU.1, C/EBPα and RUNX1. These are important to guide the most primitive lineages into committed and differentiated cells regarding myeloid path during hematopoiesis and a loss of function in them will block the hematopoietic differentiation at the hematopoietic stem cell (HSC) level.

Table 2 - Examples of transcription factor mutations in patients with AML, regarding the chromosomal location, the frequency that occur in AML patients and the most common FAB subtype associated. AML, acute myeloid leukaemia; CBFβ, core-binding factor-β; C/EBPα, CCAAT/enhancer binding protein-α; FAB, French–American–British; MLL, mixed lineage leukaemia; H3K4, lysine 4 in histone H3; MYH11, myosin heavy chain 11; PML, promyelocytic leukaemia; PU.1, transcription factor encoded by SPI1; RARα, retinoic acid receptor-α; RUNX1, runt-related transcription factor 1.

Oncofusion proteins	Chromosomal location	Mutation and effects	Frequency in AML	FAB classification	References
PML-RARα	t(15;17)	Acts as a transcriptional repressor that interferes with gene expression programs involved in differentiation, apoptosis and self-renewal. It can suppress PU.1 expression and C/EBPα.	6-7%	M3	(8); (9); (10)
RUNX1-RUNX1T1	t(8;21)	Dominant negative regulator of wild-type RUNX1, PU.1 and suppress C/EBPα expression as well.	10%	M2	(6); (11); (12)
CBFβ-MYH11	Inv(16)	Inv(16) disrupts the gene encoding the RUNX1 co-factor, core binding factor β (CBFβ). CBFβ is a small protein that allosterically regulates the ability of RUNX1 to bind to DNA and that blocks the ubiquitin-mediated degradation of RUNX1.	8%	M4	(13)
MLL-fusions	t11q23	Leukaemogenic MLL translocations encode MLL fusion proteins that have lost H3K4 methyltransferase activity. A key feature of MLL fusion proteins is their ability to efficiently transform haematopoietic cells into leukaemia stem cells.	10%	M4/M5	(14)

Kasumi1, one of the cell lines used to perform experiments, was the chosen one to represent the particular type of RUNX1-RUNX1T1 oncofusion protein. As described, Kasumi1 has a translocation that gives rise to RUNX1- RUNX1T1 protein, down-regulating C/EBPα mRNA, protein and DNA binding activity, which is crucial for the

differentiation of granulocytes. Also, two MLL-fusions of mouse models were used, MLL/AF4 and MLL/AF9 and one human MLL-fusion, MOLM-13, as well. Both Kasumi1, MOLM-13 and MLL/AF4 and MLL/AF9 are described later in *Materials and Methods*.

On the other hand, leukemias with a normal karyotype, carry mutations in genes such as FLT3, nucleophosmin NPM1 and DNMT3A (15). That can cause a loss of coordination between proliferation and differentiation in the hematopoietic progenitor cell pool.

Table 3 shows the most relevant gene mutations for this thesis with the respective chromosomal location, and their effect on AML cells.

Table 3 - Examples of gene mutations in patients with AML, regarding the chromosomal location, the frequency that occur in AML patients. AML, acute myeloid leukaemia; C/EBPα, CCAAT/enhancer binding protein-α; MLL, mixed lineage leukaemia; NPM1, Nucleo-phosmin 1; FLT3, fms like tyrosine kinase 3; ITD, Internal Tandem Duplication; BAX, BCL2-associated X protein; DNMT3A, DNA (cytosine-5)-methyltransferase 3A.

Gene Mutations	Chromosomal location	Functions and mutation effects	Frequency in AML	Representative Cell Lines	References
NPM1	Chromosome 5q35	Some functions of NPM1 protein include binding of p53, initiate centrosome duplication and ribosomal protein assembly and transport. This mutation has been reported to be involved in leukemogenesis.	25%–30% of adult AML cases.	Oci-AML3	(16,17)
FLT3-ITD	exons 14 and 15 of chromosome band 13q12	FLT3 gene encodes a class III receptor tyrosine kinase (RTK). This receptor synergizes with growth factors to stimulate proliferation of stem cells, progenitor cells, dendritic cells, and natural killer cells. ITD consists in a duplication in amino acids in the juxtamembrane (JM) domain. These repeat sequences disturb autoinhibitory activity of the JM	25% of adults and 15% of pediatric AML cases.	MOLM13, MLL-AF4, MLL-AF9	(18–21)

		domain resulting in constitutive tyrosine kinase (TK) activation, leading to leukemogenesis once TKs can no longer control cellular events like proliferation, differentiation, and cell death.			
BAX	Chromosome 19q33	This gene encodes a member of BCL2 protein family. The protein is responsible for activating apoptosis by aiding in the opening of the mitochondrial voltage-dependent anion channel to release cytochrome c. The expression of this gene is regulated by the tumor suppressor P53 and has been shown to be involved in P53-mediated apoptosis.	20% of adult AML cases.	Oci-AML3	(16,19, 22)
RAS	HRAS (11p15.5), KRAS (12p12.1), and NRAS (1p13.2)	Ras proteins belong to the super family of small GTPases and it is comprised of three homologues, HRAS (11p15.5), KRAS (12p12.1), and NRAS (1p13.2). They cycle between the active GTP-bound form and the inactive GDP-bound form. Mutations within the RAS gene result in constitutive activation of the RAS GTPase. The result is a sustained proliferation signal within the cell, even in the absence of growth factor signalling.	11% of NRAS mutations, no evidencies of HRAS, and 5% in KRAS mutations of adult AML cases.	Oci-AML3	(23,24)
DNMT3A	Chromosome 2p23	The DNMT3A gene encodes the DNA methyltransferase 3A, an enzyme that catalysis the process of de novo DNA methylation, and as such, plays a role in cancer development through deregulation of gene expression. DNMT3A mutations most often occur at the R882 residue of the protein, and they are believed to cause loss of function or may induce epigenetic changes by affecting the DNA methyl-transferase activity, which contribute to leukemogenesis.	13,5% of adult AML cases.	-	(25–27)

As previously said, mouse models MLL/AF4 and MLL/AF9 which have $FLT3^{ITD/+}$ mutation as well were used to perform experiments. $FLT3^{ITD/+}$ MLL/AF4 and MLL/AF9 are described later in Materials and Methods.

Moreover, human AML cell line, MOLM-13, carries a CBL-ΔExon8 mutation (28) which can lead to dysregulation of receptor tyrosine kinases and have the potential to transform hematopoietic cells by constitutively activating the FLT3 pathway (29). This means that MOLM-13 cell line carries an ITD mutation of FLT3 kinase as well.

Apart from those, Oci-AML3s carry also mutations in BAX and Ras proteins (see table 3).

1.2. Gene Editing

As previously stated, gene editing was utilized through CRISPR Cas9 technology in a drop-out screen for genetic vulnerabilities in AML cell lines. This work presents the same approach of CRISPR/Cas9 system genetic engineering, which offers the ability to target and study precise DNA sequences in the vast expanse of a genome. CRISPR functions as an adaptive immune system in bacteria (30), which can target specific sequences of foreign nucleic acids. It relies on Cas9 endonuclease, which cause double-stranded cleavage to any target location in DNA sequence, determined by a single guide RNA (sgRNA) and can lead to a specific gene knockout (KO), by stopping the transcription of the target gene (31). Figure 1 schematizes the CRISPR/Cas9 system and the target gene recognition.

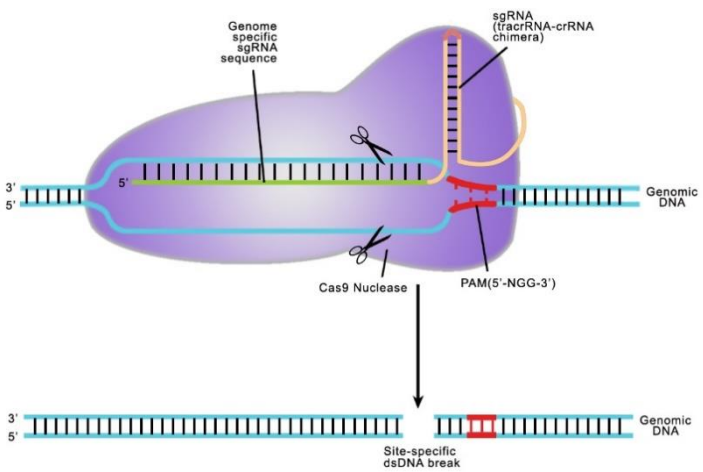

Figure 1 *- CRISPR-Cas9 target recognition. The sgRNA (in green) hybridizes with the strand opposite the PAM site (in red), where the transcript RNA (in yellow) is important to binding the Cas9 protein. After, the Cas9 nuclease cuts the DNA, giving rise to a site-specific double strand DNA (dsDNA) break. Ref: Moore, C.B. et al., 2010* (32).

Moreover, we took advantage of another system, in order to achieve a target gene knockdown instead of a knockout, and it was possible through the technology of short hairpin RNAs (shRNA). shRNAs are sequences of RNA that include a region of internal hybridization that creates a tight hairpin structure which can be used to silence target gene expression via RNA interference (RNAi). Expression of shRNA in cells can be achieved by plasmids delivery or through infection of the cell with virally produced vectors (33). Lentiviral delivery of the shRNA enables stable expression and permanent knockdown of the target gene. After the vector integrates the host genome, shRNA is formerly transcribed in the nucleus by polymerase III from U6 promoter in the nucleus. The product, pri-miRNA, is processed by Drosha (class II ribonuclease enzyme) into a hairpin shaped precursor miRNAs (pre-miRNA). The resulting pre-miRNA is exported to the cytosol by nuclear export receptor Exportin 5. This product is then processed by the endoribonuclease enzyme Dicer, which converts the shRNA into the siRNA duplexes (34), and loaded into the RNA-induced silencing complex (RISC). The sense strand is rapidly destroyed and the antisense, which is the guide strand, directs RISC to mRNA that has a complementary sequence. In the case of perfect complementarity, RISC cleaves the mRNA. In the case of impaired complementarity, RISC supresses translation of the mRNA. In both cases, shRNA leads to target gene silencing (35,36)(Figure 2).

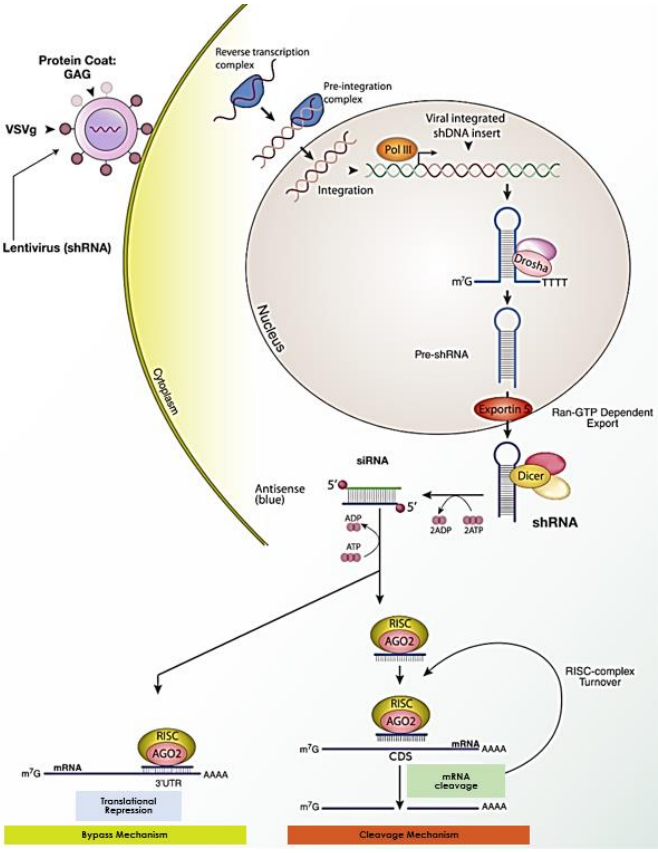

Figure 2 *– shRNAs mechanism. Lentiviral delivery and machinery of RNA interference (iRNA) in mammalian cells until the last step of translational suppression or mRNA cleavage. GAG indicates glycosaminoglycans; VSVg, component of vector envelope. Ref: Cojocari, D., 2010* (37).

1.3. Acute Myeloid Leukemia and MAT2A

Methionine adenosyltransferase 2A, known as *MAT2A*, a subunit of *MAT2* enzyme, utilizes L-methionine (Met) and adenosine 5′-triphosphate (ATP) to form SAM (S-adenosyl-L-methionine), the universal methyl donor for methylation reactions, like histone and DNA methylation, for instance. This event befalls in a three-part cycle represented in Figure 3, where the folate and the methionine cycles are presented, together with histone methylation. In this last one, histone methyltransferases (HMT) donate the SAM methyl group to their histone substrates, producing S-adenosylhomocysteine (SAH). In turn, SAH is hydrolysed to homocysteine (hCys) and to complete the cycle, hCys is then metabolized through two major pathways: methylation and transsulfuration (38). Under normal conditions, approximately 50% of hCys is re-methylated

to form methionine which, in most tissues, occurs via methionine synthase (MS) by donation of a methyl group from 5-methyltetrahydrafolate (5-mTHF)(39) or hCys may also be converted to methionine via betaine–homocysteine S-methyltransferase (BHMT), which is predominantly present in the liver (40) (see Figure 3).

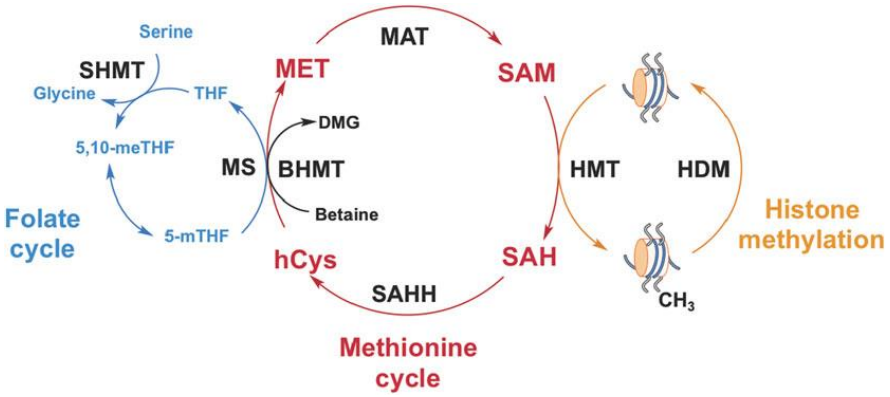

Figure 3 *- One-carbon metabolism and histone methylation. Methionine adenosyltransferase (MAT) uses methionine (MET) to form S-Adenosylmethionine (SAM) and histone methyltransferases (HMTs) utilize SAM to donate a methyl group to their histone substrates. While histone demethylases (HDMs) remove the methyl group from histones now methylated, the resulted S-adenosylhomocysteine (SAH) is converted to homocysteine (hCys) via S-adenosylhomocysteine hydrolase (SAHH). In turn, hCys can be remethylated to regenerate MET by donation of a methyl group from 5-methyltetrahydrafolate (5-mTHF) via methionine synthase (MS) or from betaine via betaine–homocysteine S-methyltransferase (BHMT).*
Ref: Mentch, S.J., Locasale, J.W., 2015 (39)

The trans-sulfuration pathway, Figure 4, involves the interconversion of hCys, through the intermediate cystathionine, by CBS (cystathionine β-synthase), which is the immediate precursor to cysteine. Cysteine is utilized in the synthesis of glutathione, a tripeptide that reduces reactive oxygen species (ROS), thereby protecting cells from oxidative stress (41). This is important as, depending on demand, metabolism of homo-cysteine can be redirected to increase methylation potential, by producing methionine, or towards trans-sulfuration pathway, producing antioxidants.

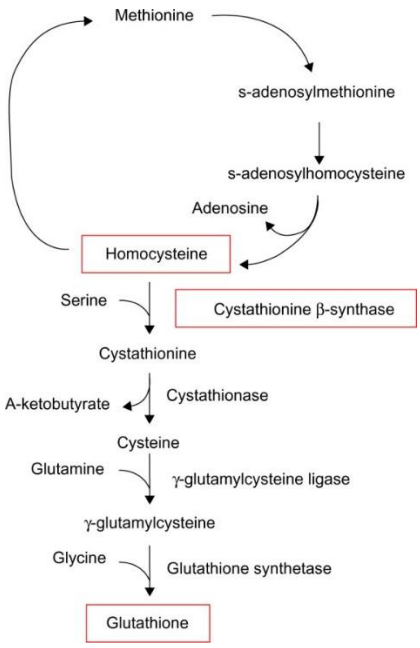

Figure 4 *- Methionine cycle and trans-sulfuration pathway. Glutathione synthesis starts with the conversion of homocysteine into cystathionine, which is dependent on the presence of both serine and cystathionine β-synthase. Cystathionine origins cysteine by cystathionase and with a loss of a- ketobutyrate. In turn, cysteine origins γ-glutamylcysteine with the use of glutamine and γ-glutamylcysteine ligase, and finally, depending on glycine and glutathione synthetase, glutathione is formed.*
Ref: Adapted from: Hitchler, M.J., Domann, F.E., 2007 (42).

Focusing on the methionine downstream product, S-Adenosylmethionine (SAM), it is the principal methyl donor in the cell. Epigenetic modifications, such as histone modifications, are important in the establishment of chromatin states that control gene expression and DNA accessibility. Those are crucial to normal development and differentiation of distinct cell lineages in the adult organism. SAM donates methyl residues for methylation of DNA, RNA, proteins and lipids by a variety of methyltransferases. MAT is thus a critical cellular enzyme that catalyses SAM production from methionine and participates in key metabolic pathways.

Almost 60 years ago, Sugimura *et al*. (43) indicated that methionine metabolism is fundamental for cancer cell proliferation. There is direct evidence that noncancerous cells can thrive without methionine, while in various cancers, cells cannot, even when hCys is present (44,45). The higher the metastatic potential of the cell line, the higher the concentration of methionine required to maintain its proliferation (46). The mechanisms responsible for methionine dependence in malignant cell lines are not fully un-

derstood but it is known that methionine-dependent cells endogenously synthesize methionine at normal levels in homocysteine media but show reduced SAM synthesis (4). Also, when SAM is added to hCys medium, methionine-dependent breast cancer cells could proliferate, implying that some cancer cells are especially sensitive to SAM limitation (47).

There are two forms of MAT (see Figure 5): MAT I/III that is encoded by the MAT1A gene and is expressed in the liver; and MATII, encoded by MAT2A, which is widely distributed in non-hepatic tissues and which enzymatic activity is regulated by an associated subunit, MAT2B (48,49). MAT2A is thus the primary enzyme catalysing SAM production in most cell types, including cancer cells, and also during development, including in the developing fetal liver, where MAT2 predominates. Progressively, fetal liver MAT2 is replaced by the liver-specific isoforms during development (50).

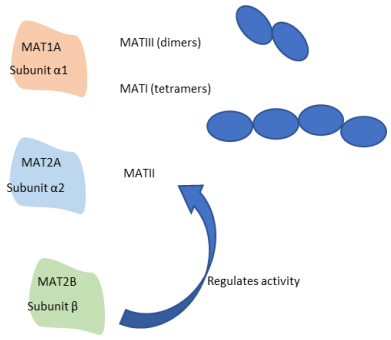

Figure 5 *– Dimeric composition of MAT enzyme. MAT1A and MAT2A encode two MAT catalytic subunits, α1 and α2, correspondingly. The α1 subunit organizes into dimers (MATIII) or tetramers (MATI). The α2 subunit is found in the MATII isoform. A third gene MAT2B, encodes a regulatory subunit β, that regulates the activity of MATII. Adapted from: Cai, J., et al., 1998* (51)

MAT2A plays an important role in solid cancers. It was shown that a switch in *MAT* expression in liver, from *MAT1A* to *MAT2A*, played an important pathogenic role in promoting liver cancer growth (52) and that silencing of *MAT2A* expression resulted in inhibition of cell growth and induction of apoptotic cell death in human hepatoma cells (53). Similar to the liver, overexpression of *MAT2A* has been found in other human solid tumors, including colon cancer (54) and breast cancer (55).

A CRISPR Drop-out Screen of genetic vulnerabilities in human AML cell lines published collaboratively by the Pina lab (22) identified *MAT2A* as being required for AML maintenance in 4 out of 5 cell lines (figure 6).

Figure 6 *- Schematic representation of results of the Tzelepis et al CRISPR/Cas9 drop-out screen for MAT2A, evidencing the need of MAT2A for maintenance of AML cell lines. Significant p-values for gene drop-out represented in colour at different levels of FDR (yellow<20%; gold<10%; orange<5%; brown<1%); grey, not significant. Adapted by Pina lab from Tzelepis K., et al., 2016* (22).

MAT2A role in leukemia, particularly AML, has not been explored to date. Given the importance of MAT2A for solid cancer development, I undertook validation of the screen results in AML cell lines representative of common forms of human disease.

2. Objectives

The overarching goal of the research presented in this thesis is to extend the knowledge on the role of the MAT2A gene in Acute Myeloid Leukemia. To achieve this goal, I ablated expression of MAT2A in three human AML cell lines (Kasumi1, MOLM13 and Oci-AML3) and two transformed MLL-AF4 $FLT3^{ITD}$ and MLL-AF9 $FLT3^{ITD}$ primary mouse bone marrow (BM) and evaluated consequences in terms of growth and survival of leukemic cells.

3. Materials and methods

3.1. Cell lines

3.1.1. Mouse Cell Lines

Mouse cell lines were obtained from FLT3$^{ITD/+}$ mice background (20). These bone marrow cells were further engineered to express Cas9, by inserting the human EF1α promoter-driven Cas9 expression cassette, using a ubiquitous promoter, Rosa26 promoter (22).

The Cas9 FLT3 $^{ITD/+}$ cells were then transformed by introducing a retrovirus construct expressing either MLL/AF9, pMSCV-MLL-AF9-IRES-YFP (56) or MLL/Af4, pMSCV-MLL-AF4-PGK-puro (57). Afterwards, the cells were transplanted into recipients that were allowed enough time to develop leukemia (22). Leukemic cells from these mice were isolated, kept in culture, and consequently frozen. Cells were thawed and placed in culture accordingly with experimental needs, as described below.

3.1.2. Human Cell Lines

MOLM-13 cell line was established from the peripheral blood of a 20-year-old man with acute myeloid leukemia AML classified as a M5, accordingly to French–American–British classification (FAB) (58).

Oci-AML3 cell line was established from the peripheral blood of a 57-year-old man with acute myeloid leukemia classified as a FAB M4, accordingly to French–American–British classification, at diagnosis in 1987 (58).

Kasumi1 cell line was established from the peripheral blood of a 7-year-old Japanese boy suffering from acute myeloid leukemia (AML). This is a leukemic cell line with an 8;21 chromosome translocation, that has characteristics of myeloid and macrophage lineages and it is classified as a FAB M2, accordingly with FAB classification (59). This translocation juxtaposes the RUNX1 with RUNX1T1 gene, which leads to chimeric RUNX1 – RUNX1T1 protein production. This protein down-regulates C/EBPα mRNA, protein and DNA binding activity, which is crucial for the differentiation of granulocytes (60).

Last of all, epithelial 293T cell line is a highly transfectable derivative of human embryonic kidney 293 cells and contains the SV40 T-antigen, which means it is competent to replicate vectors carrying the SV40 region of replication. This embryonic kidney cell line, also called HEK293, is an adherent cell line, allowing the viral particles to be collected from the culture medium. It has been widely used for high-titer retroviral production, gene expression and protein production. To run the experiments, constructs that expressed retroviral packaging functions were stably introduced into 293T cells (61).

3.2. Cell Culture

FLT3 MLL/AF4-Cas9 and FLT3 MLL/AF9-Cas9 cell lines were cultured in RPIM 1640 (Roswell Park Memorial Institute 1640 Medium, Sigma-Aldrich) supplemented with 20% FBS (Fetal Bovine Serum, Sigma-Aldrich), 1% penicillin/streptomycin ([peniciline]=100 units/mL and [streptomycin]=100µ/mL from Sigma-Aldrich) and 1% L-glutamine (in a final concentration of 2 mM, from Sigma-Aldrich), in the presence of 10 ng ml^{-1} mIL-3 (Peprotech), added every other day to the culture. This cytokine would stimulate the cells to grow. These cell lines were cultured and divided into the final concentration of 3 x 10^5 cell mL^{-1} and were incubated at 37 ºC and 5% CO_2.

MOLM13, Oci-AML3 and Kasumi1 AML human cell lines were cultured in RPIM 1640 (Sigma-Aldrich) supplemented with 20% FBS (Sigma-Aldrich), 1% penicillin/streptomycin ([peniciline]=100 units/mL and [streptomycin]=100µ/mL from Sigma-Aldrich) and 1% L-glutamine (in a final concentration of 2 mM, from Sigma-Aldrich). MOLM13 and Oci-AML3 cell lines were cultured and divided into the final concentration of 5 x 10^5 cell mL^{-1} and were incubated at 37 ºC and 5% CO_2. Kasumi1 line was cultured and divided into the final concentration of 0.7 x 10^6 cell mL^{-1} and was incubated at 37 ºC and 5% CO_2. Lastly, K652 cell line was cultured and divided into the final concentration of 0.7 x 10^5 cell mL^{-1} and was incubated at 37 ºC and 5% CO_2. All cancer cell lines were obtained from the Sanger Institute Cancer Cell Collection and negative for mycoplasma contamination (22).

293T/human embryonic kidney (HEK) cells, used to produce lentiviral constructs, were maintained in DMEM (Dulbecco's Modified Eagle's Medium, Invitrogen) supplemented with 10% FBS (Invitrogen), 1% Penicillin/Streptomycin ([peniciline]=100 units/mL and [streptomycin]=100µ/mL from Sigma-Aldrich) and 1% L-glutamine (in a final concentration of 2 mM, from Sigma-Aldrich).

3.3. Plasmid construction

3.3.1. pKLV2 vector for guideRNA.

A lentiviral backbone vector, pKLV2, was previously generated in the study of "A CRISPR Dropout Screen Identifies Genetic Vulnerabilities and Therapeutic Targets in Acute Myeloid Leukemia" by Konstantinos Tzelepis and a partnership of Pina's lab group (22). The plasmid pKLV-U6gRNA(BbsI)-PGKpuro2ABFP has been deposited with Addgene (ref: 50946).

Guide RNAs are expressed through a RNA polymerase III U6 promoter. Integration of the gRNA is reported from the PGK (phosphoglycerate kinase) promoter, which is correlated with BFP (Blue Fluorescent Protein) expression cassette. Ampicillin resistance cassette is also present, which makes sure these plasmids can grow in an environment containing ampicillin, needed when cloning gRNAs (see Figure 7A). In order to insert guides for mouse Mat2a gene or human MAT2A gene, pKLV2 plasmid was previously digested (by Pina's lab group) with BbsI in two sites giving rise to two sticky ends (see Figure 7B).

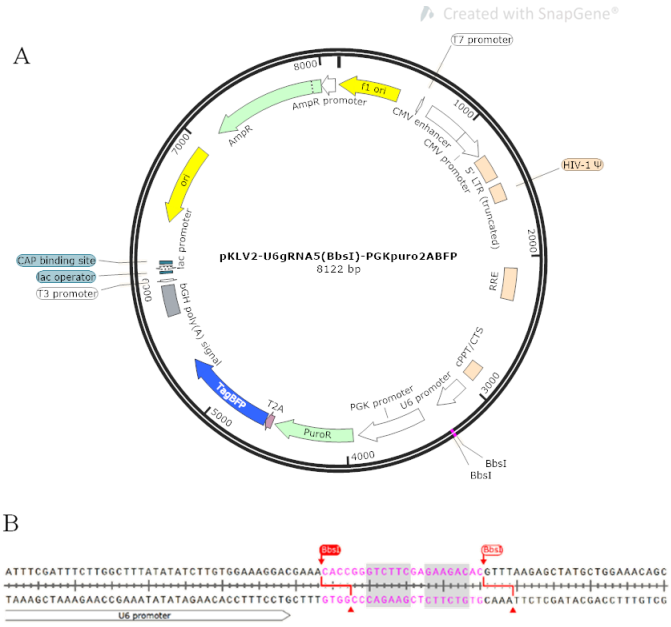

Figure 7 *- A) Design of pKLV2 vector. Expresses gRNA under the pol III U6 promoter. The plasmid contains a PGK promoter cassette to monitor expression of gRNAs. The bacterial plasmid is resistant to ampicillin, since the AmpR cassette is present. Restriction enzymes BbsI cut two sticky ends, which are responsible to attach the designed gRNAs, complementary to the restriction ends. B) Excerpt of pKLV2 plasmid sequence where we can see the sequencing cut recognized by BbsI restricted enzymes, creating two sticky ends that bind guideRNAs for Mat2a and MAT2A genes. Figures created with SnapGene ® Viewer 3.3.3 program.*

3.3.2. LentiLox 3.7 vector for short hairpin RNA (shRNA).

pLL3.7 (LentiLox 3.7) lentiviral vector, obtained beforehand, expresses shRNAs from a Polymerase III U6 promoter. Incorporation of the shRNA is reported from the CMV (cytomegalovirus) promoter, which is observed by GFP (Green Fluorescent Protein) expression cassette, that is correlated with shRNA expression. Ampicillin resistance cassette is also present, which makes sure these plasmids can grow in an environment containing ampicillin, needed when cloning gRNAs (see Figure 8A). The plasmid was digested with *XhoI* and *HpaI* restrict enzymes, using 1X CutSmart® Buffer (New England Biolabs, NEB). Restriction enzyme *HpaI* cuts the 3' cloning site bluntly, where *XhoI* leaves a sticky end when cutting the 5' cloning site, open for binding of the designed oligos to complement the restriction ends (see Figure 8B).

After an incubation of 3h at 37°C, a 0.8% agarose gel was run for purification in 1x TAE (Tris-acetate-EDTA, CIMR). SYBR Safe Gel Stain (Invitrogen) was added to

enable DNA visualization. A mix of 50 µL of the digested vector DNA with 10 µL loading dye (5x, QIAGEN) were loaded into the agarose gel divided between two wells. The gel was run for 2h and thereafter, linearized DNA was cut out from the gel and further purified using QIAquick Gel Extraction Kit (QUIAGEN) (see Annexes, 7.2.). A non-digested negative control was used (see Figure 20 in results).

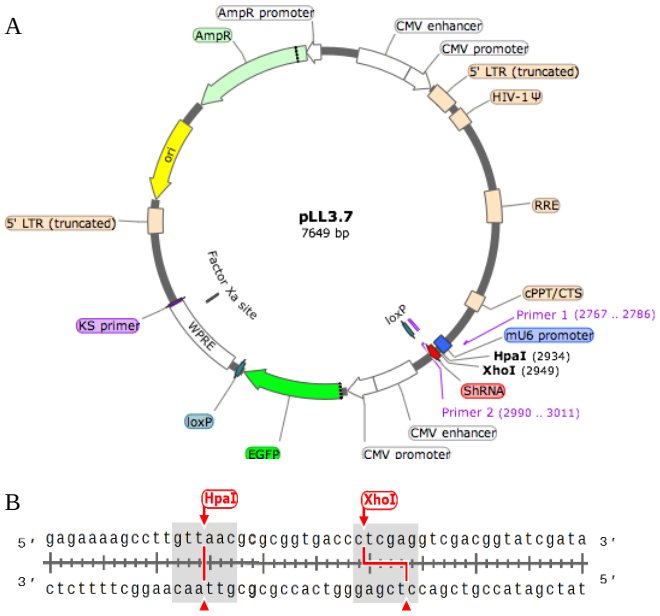

Figure 8 *- A) Design of pLL3.7 vector. Expresses shRNA under the pol III U6 promoter. The plasmid contains a CMV promoter cassette to monitor expression of shRNA. The bacterial plasmid is resistant to ampicillin, since the AmpR cassette is present. Restriction enzymes HpaI cuts the 3' cloning site bluntly, where XhoI leaves a sticky end when cutting the 5' cloning site, open for binding of the designed oligos to complement the restriction ends. B) Exert of Pll3.7 plasmid sequence where we can see the cut sequencing recognized by restricted enzymes. Figures created with SnapGene ® Viewer 3.3.3 program.*

3.4. gRNA and shRNA design

3.4.1. gRNAs

Individual gRNA expression vectors were previously designed by Pina's group lab as follows. 24-nt human and 23-nt mouse oligonucleotides (Sigma-Aldrich) (see

tables 1 and 2) were reconstituted with DEPC-Treated Water to the stock concentration of 100µM. gRNA were design to fit and attach in the linearized pKLV2 vector. So that, Forward oligos should start with CACCG from 5' to 3'. On the other side, the Reverse oligos should start at AAAC from 5' to 3'. This way, the ds-oligos would attach to the pKLV2 plasmid, as we can observe in Figure 1 (pKLV2 plasmid when cut with BbsI).

Table 4 *- Sequences (5'-3') of forward (Fw) and reverse (Rv) guides for human MAT2A gene.*

Human Guides		**Sequences (5'-3')**
gMAT2A - 1	Fw	CACCGAGTCACCAGATATTGCTCA
	Rv	AAACTGAGCAATATCTGGTGACTC
gMAT2A - 2	Fw	CACCGCACAAGCTAAATGCCAAAC
	Rv	AAACGTTTGGCATTTAGCTTGTGC
gMAT2A - 3	Fw	CACCGTTACTTGAGTTTTAGAATC
	Rv	AAACGATTCTAAAACTCAAGTAAC
gMAT2A - 4	Fw	CACCGTGCAGTATATGCAGGATCG
	Rv	AAACCGATCCTGCATATACTGCAC
gMAT2A - 5	Fw	CACCGGTTTGTCTTGATGAAATGA
	Rv	AAACTCATTTCATCAAGACAAACC

Table 5 *- Sequences (5'-3') of forward (Fw) and reverse (Rv) guides for human MAT2A gene.*

Mouse Guides		**Sequences (5'-3')**
gMat2a - 1	Fw	CACCGAGAATCTGGGCGTAACCA
	Rv	AAACTGGTTACGCCCAGATTCTC
gMat2a - 2	Fw	CACCGACAAGCTAAATGCCAAAT
	Rv	AAACATTTGGCATTTAGCTTGTC
gMat2a - 3	Fw	CACCGCGGTCAAGATGAACACCT
	Rv	AAACAGGTGTTCATCTTGACCGC
gMat2a - 4	Fw	CACCGGTCACCAGATATTGCCCA
	Rv	AAACTGGGCAATATCTGGTGACC
gMat2a - 5	Fw	CACCGAGAAACTGTTGCTAAAAC
	Rv	AAACGTTTTAGCAACAGTTTCTC

3.4.2. shRNAs

Short hairpin RNAs were constructed to fit in our lentiviral backbone for later transduction of Oci-AML3, MOLM13. shRNAs had to be read by a polymerase III promotor. Two short hairpin RNAs were designed for MAT2A gene, to increase the probability of knockdown. Oligo's were synthesized (Sigma-Aldrich) with the following sequence:

MAT2A sh1: 5’-

TAGCAGTTGTGCCTGCGAAATAGGGATCCTATTTCG-CAGGCACAACTGCTTTTTTTC-3’

MAT2A sh2: 5’-

TGTTCAGGTCTCTTATGCTATTGGGATCCAATAGCATAAGAGAC-CTGAACTTTTTTC-3’

In order to fit the lab’s shRNA library, few variations were made in the hairpins from Sigma-Aldrich library: The start base was adjusted from CCGG to T; the loop sequence was adjusted from CTCGAG to GGGATCC (recognized by BamHI restriction enzyme) and one T-base was added to the poly T-tail.

Both forward and reverse oligos were reconstituted with DEPC-Treated Water, to the stock concentration of 100µM.

3.5. Cloning gRNA and shRNAs: annealing, ligation and transformation

The following protocol was individually used for both gRNAs or shRNA.

1.2 µL of each sense and antisense oligonucleotides were annealed with 1µL of EcoRI buffer (NEB) and DEPC-treated water to perform a 10 µL reaction. The reactions were placed in a PCR (Polymerase Chain Reaction) machine, thermal cycler (G-Storm GS0004M). The program was set to start at 95 °C for 4 min, followed by 70°C for 10 min and then ramped down to 20 °C at 0.1 °C/sec, ending at 4 °C for 10 min.

The annealed ds-oligos, gRNAs and shRNAs, were then ligated into the BbsI site of an already linearized pKLV2-U6gRNA(BbsI)-PGKpuro2ABFP (previously digested with BbsI) and into the digested (with XhoI and HpaI) vector pLL3.7, respectively. The ligation reaction was established using 1µL of enzyme T4 Ligase (BioLabs), 1µL of 10X buffer for T4 ligase (BioLabs), 1 µL of linearized backbone in the case of pKLV2 and 2 µL of linearized backbone in the case of pLL3.7, 5µL of the annealed oligos and DEPC-water to make up a 10µL reaction. Two controls were made, one by

adding H_2O instead of ds-oligos, which quantifies incompletely digested and re-ligate vectors. In the other control, H_2O was used to replace the T4 ligase, which can cross out the undigested vectors. The reactions were left incubating overnight at room temperature.

Afterward, 2µL of ligation products were transformed individually into 15µL aliquot of competent Cells (NEB® Stable Competent E. coli (BioLabs) for pKLV2 plasmid and Stellar Chemically Competent Cells (Clontech) for pLL3.7 plasmid). The competent cells were incubated on ice for 30 minutes, followed by a heat shock at 42 °C for 30 seconds and returned on ice for 2 minutes. To those cells were added 200 µl of Lysogeny broth (LB) broth media, where they were left incubating for 1 hour at 30-37°C and 250 rpm in a Thermo-Shaker (Grant-bio, PCMT), which allowed the cells to recover.

200 µL of transformed bacteria with pKLV2 plasmid and 80 µl of culture with pLL3.7 plasmid were then plated on LB-agar plates containing 100 µg/mL ampicillin and they were incubated overnight at 37ºC. If transformation was successful, meaning there were few bacterial colonies in the controls compared with the sample colonies, 3-8 bacterial colonies were inoculated into 5 mL LB with 5 µL ampicillin, using inoculation loops (Nunc™) and were incubated overnight at 37°C, 225 rpm, which allowed the cells to recover.

Bacterial colonies were then miniprepped to isolate plasmid DNA using QIAprep® Spin Miniprep Kit 50 (QIAGEN), (see Annexes, 7.1.). Ultimately, DNA concentration was measured by NanoDrop Lite Spectrophotometer (Thermoscientific).

3.5.1. Glycerol stocks

In Eppendorf® Safe-Lock microcentrifuge tubes of 2 mL with 150 µL of glycerol 99%, was added 850 µL of bacterial culture. The mixture was vortexed a few seconds and was immediately frozen and kept at -80 ºC.

3.6. Screen for positive clones

3.6.1. gRNA clones – BbsI digestion

A first screen was performed prior to sequencing: digestion reactions with BbsI were established to each gRNA sample in order to exclude the non-digested samples, as those ones would not have the gRNA oligos incorporated. If the samples were positive, BbsI would not cut the plasmid, because once the gRNAs are incorporated, BbsI restriction site is no longer present. In figure 13 in results we can see all the samples are positive, as BbsI enzyme could not cut the plasmid, as it did with positive control.

Digestion reactions were set up using a MasterMix (MM) containing (per reaction): 0.5µL of BbsI enzyme (Thermo Scientific), 2 µL of G buffer (10x buffer Thermo Scientific) and 7.5 µL of water/per reaction. The MM was then combined with 10 µL of each DNA sample in a concentration of approximately 150 ng/µL. Two controls were made: a negative control with a DNA sample without the sequence recognized by the BbsI enzyme (5' GAAGAC 3', 3' CTTCTG 5') and a positive control. The samples were incubated at 37 °C and after one hour, the temperature increased up to 65°C for 20 min to inactivate the BbsI enzyme. Afterwards, the samples were run on a 0,8% agarose gel in 1x TAE (Tris-acetate-EDTA, CIMR) with a DNA ladder as reference (BioLabs) (see Figure 13 in results). SYBR Safe DNA gel stain (Invitrogen) was added to the gel to enable DNA visualization. Two positive clones for each gRNA were sent for sequencing to Source Bioscience Sequencing, using the pKLV Forward Primer with the sequence: CGATACAAGGCTGTTAGAG, in a concentration of 3.2 µmol/µL.

3.6.2. shRNA clones – PCR screening and BamHI digestion

The isolated bacterial plasmid DNA was screened for successfully ligated clones by PCR, making use of the ThermoCycler (G-Storm GS0004M). Primers were used as follows: Forward primer- CTGTTCTTTTTAATACTAGC, and Reverse primer: TATTAGGTCCCTCGACCTGCTGG, represented as Primer 1 and 2 respectively in Figure 2.

PCR reactions were set up by making a MM containing (per reaction): 10 µL Taq MasterMix (QIAGEN), 1 µL of each primer (fw and rv, 100 µM stocks) and 7.5 µL

RNAse free water. 19.5 µL of the MM was added to the PCR tubes and 0.5 µL of the miniprepped DNA for each different clone was added. Per PCR three controls were required: a blank control using RNAse free water instead of plasmid DNA to check for contamination; a positive control using 0.5 µL of the LLX-vector containing a shRNA to recognize positive clones and a negative control using 0.5 µL of the original vector to distinguish negative clones. Thermocycler settings used were as follows: 94°C for 3 min, 40x [94°C for 30 s, 57°C for 30 s, 72°C for 1 min] and lastly 72°C for 10 min. Thereupon, multiplied DNA was run on a 2% agarose gel at 50 volts for visualization with a DNA ladder (Biolabs), and the gel results are represented in figure 21 in results.

Also, digestion reactions were set up using a MM containing (per reaction): 0.5µL of BamHI enzyme 20.000U/Ml (NEB – New England Biologicals), 2 µL of buffer 3.1 10X (NEB – New England Biologicals). DNA in a concentration between 600-700 ng/uL and RNasefree water were added to a final volume of 20µL per reaction. Two controls were made: a negative control (pLLx3.7 RNA; 235.5 ng/µL): DNA sample without the loop sequence recognized by the BamHI enzyme (5' GGGATCC 3') and a positive control (LLX CTRL; 624.5 ng/µL): DNA sample with a short hairpin sequence recognized by BamHI enzyme. The samples were incubated 1h30min, at 37 °C, before running on a 0,8% agarose gel with 1x TAE (Tris-acetate-EDTA, CIMR) with a DNA ladder (BioLabs). SYBR Safe DNA gel stain (Invitrogen) was added to the gel to enable DNA visualization. Resulted gel is represented in figure 22. Four positive clones for each shMAT2A were sent for sequencing to Source Bioscience Sequencing, using the Fw (CTGTTCTTTTTAATACTAGC) and Rv (TATTAGGTCCCTCGACCTGCTGG)-primers in a concentration of 3.2 µmol/µL.

3.7. Isolation of bacterial plasmid DNA

3.7.1. gRNA clones

The clones with a positive sequencing result were therefore transformed again, using 0.5 µL of DNA and 5 µL of NEB-Stable cells. Thenceforth following the transformation protocol as described above. After the two days incubation at room temperature, a single colony was inoculated in 3 mL of LB, containing 3 µL ampicillin (final concentration of 100µg/mL) and incubated overnight at 37°C, 225 rpm. 3 mL of bacte-

rial suspension was transferred to an Erlenmeyer flask with 50 mL of LB and 50 µL of ampicillin and was incubated again overnight at 37°C, 225 rpm. To isolate bacterial plasmid DNA a Midiprep (Invitrogen) was performed (see Annexes, 7.3.).

3.7.2. shRNA clones

The clones with a positive sequencing result were therefore midipreped (Invitrogen) (see Annexes7.3.) to isolate bacterial plasmid DNA. In shRNA experiment glycerol stocks mentioned above were used.

3.7.3. DNA quantification

DNA concentration was measured by NanoDrop Lite Spectrophotometer (Thermoscientific). Once isolated, DNA should be assessed for both concentration and integrity/quality. DNA concentration (in ng/µL) should be determined by 260 nm absorbance. The purity of the RNA is determined by the 260 nm (A260) and 280 nm (A280) ratio (A260/A280). The DNA purity should preferably be between ratios of 1.8 for DNA and 2.0 for RNA.

3.8. Lentivirus production and transduction

1.28 µg of pCMV 9.81 (packaging plasmid) and 1.28 µg of pMD2G (envelop plasmid) (Addgene) were added to 1.92 µg of pKLV2 vector with the gRNA or shRNA of interest, per flask equivalent. Once the reactions were settled, with TE (Tris-EDTA) buffer until a 9.3 µL volume, the DNA mixes were added to the transfection agents (237 µL Optimem and 15,8 µL transIT per flask to transfect) and were incubated for 20-30 minutes at room temperature. After that, the solutions were separately wisely dropped into T75 flasks, cultured with 293T cells attached on one surface with 8 mL of DMEM (D10) media. After swirling the flasks, they were left incubating at 37°C and 5% CO_2. Viral supernatant was harvested 48h and 96h after transfection, centrifuged at 400g for 5 minutes to discard spliced cells and the remained supernatant was centrifuged again overnight at maximal speed (3200 rpm), 4°C, acceleration 6 and deceleration 2. The

medium was replaced with fresh DMEM media (8 mL) 24h after transfection. Virus were then re-suspended in preferably 30 µL per flask equivalent.

3.8.1. Viral Transduction with guide RNAs

Delivery of viral of gmMat2a and empty vector was achieved by Viral Transduction of FLT3 MLL/AF4 Cas9 and FLT3 MLL/AF9 Cas9. Experimental set up was performed in 24-well plates with 3 x 10^5 cells/well and viral supernatant were added to 1 mL of culture medium as follows: 1 flask equivalent of empty vector and 1/5 flask equivalent for mMat2a guides (a set of 5 guides). Cells were incubated for an overnight period at 37°C, 5% CO_2.

Delivery of viral of gMAT2A and empty vector was achieved by Viral Transduction of MOLM13, Oci-AML3 and Kasumi1 cell lines.

Related to MOLM13 and Oci-AML3, experimental set up was performed in 48-well plates with 5 x 10^5 cells and viral supernatant were added to 500 µL of culture medium as follow: 1 flask equivalent of empty vector and 1/3 flask equivalent for empty vector and MAT2A guide.

In the transduction of Kasumi1 experimental set up was performed in 48-well plates with 1 x 10^5 cells and viral supernatant were added to 500 µL of culture medium as follow: 2 flasks equivalent of empty vector and 1/2 flask equivalent for each MAT2A guide.

Lastly, cells were incubated for an overnight period at 37°C, 5% CO_2.

3.8.2. Viral transduction with short hairpin RNAs for MAT2A gene

Delivery of viral of shMAT2A and shCTRL was achieved by Viral Transduction Transduction of Oci-AML3 cells. Experimental set up was performed in 24-well plates with 5 x 10^5 cells and viral supernatant were mixed in 1 mL of culture medium as follows: 1.5 flask equivalent of shCTRL, of 48h and 96h after collection, separately, and

1.5 flask equivalent for shMAT2A, in duplicate as well, using the 48 h and 96 h collection.

Subsequently all transduced cells were incubated overnight at 37°C and after transduction, cells were washed 2 times with PBS (Phosphate-buffered saline buffer) (Sigma-Aldrich) and once with Culture media, further placed in culture as mention above. Cells controls were made for each cell line. The lentiviral vector that carries the guide also expresses BFP as a reporter, so that transduction efficiency was quantified by Flow cytometry analysis.

3.9. FACS and FACS-sorting

After washing, cells transduced with guideRNAs were analyzed by a fluorescence-activated cell sorting (FACS) for BFP expression in a flow cytometry (Gallios, Beckman Coulter) to evaluate the efficiency of the transduction, since the lentiviral system uses blue fluorescent protein (BFP) as a reporter. Cells transduced with shRNA were analyzed for GFP expression. To analyze, 50 µL of each sample were supplemented with 200uL of MOJO-buffer 1x (BioLegend). A negative control was used to set the gating strategy, as we can see in Figure 9.

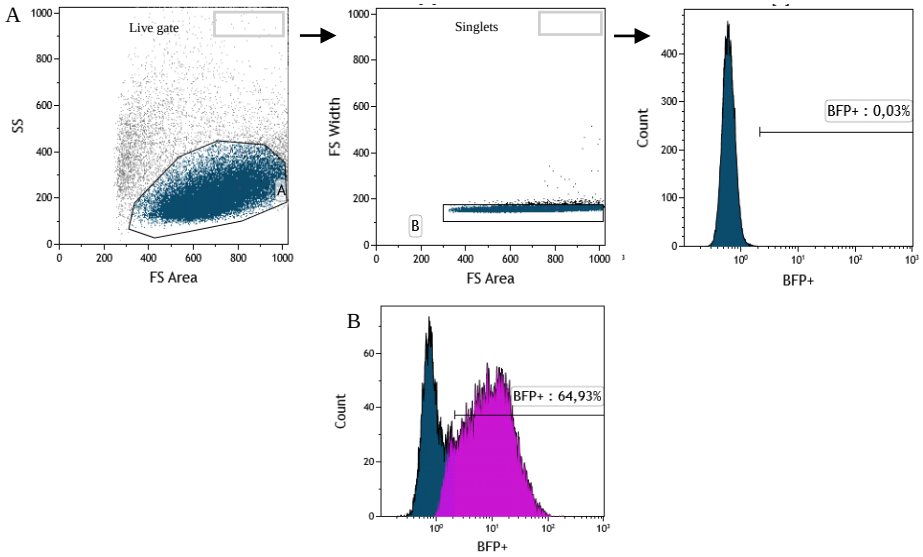

Figure 9 *- Example of sort plots. A) Gating strategy for Gallios flow cytometry. First histogram shows a gate to select living cells, through forward scatter-FS and side scatter-SS. FS detects cell size and SS*

determines the granularity and complexity of the cell. To exclude doublets, a second gate was established contemplating only living cells (SS Width vs. SS Area). Then, singlets were gated on BFP positivity. The third histogram shows the negative control, with uninfected cells, in which we based to determine the negative population for BFP positive. B) Example of a BFP positive population, that shows the percentage of transduced cells. These graphs resulted from MOLM13 cells.

Upon confirmation of the presence BFP positive population, samples were sorted in order to obtain the BFP+ cell population. Again, in case of shRNAs, the cells were sorted for GFP expression, instead of BFP.

Cell suspension were span down at 2000 rpm for 5 min and the supernatant was discarded. Cell pellets were resuspended in MOJO buffer 1x (BioLegend) and transferred into sort tubes. Oci-AML3, MOLM13 and Kasumi1 cell lines were filtrated before sorting. The cells were sorted using BD INFLUX sorter. BFP and GFP positive cells were sorted into R20 media. All FACS analyses were performed on Kaluza Analysis (Beckman coulter).

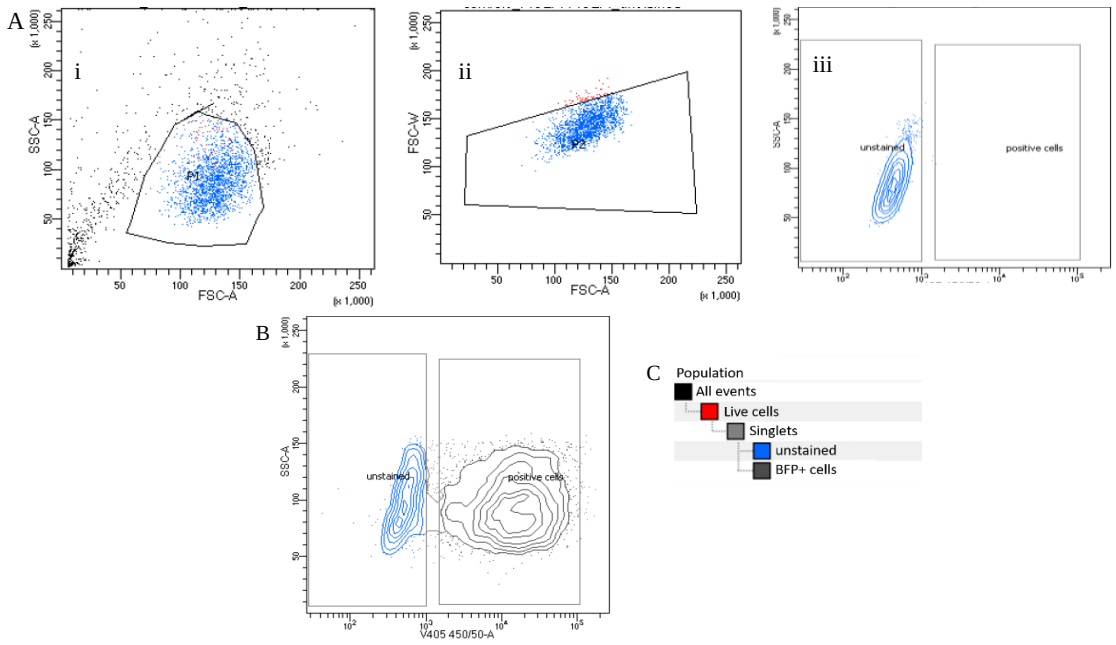

Figure 10 *- Example of FACS analysis and sort of living cells transduced with BFP. A) Gating selection using a negative control unstained. i. shows the gate for live cells (SSC-A vs. FSC-A). ii. From these a second gate was drawn to separate singlets from doublets (FSC-W vs. FSC-A). iii. Singlets were gated for BFP positivity. B) Example of a BFP+ population being sorted. C) Scheme that shows all different cells*

in the culture. All histograms correspond to MOLM13 cells; A- MOLM13 CTRL, B- MOLM13 transduced with gMAT2A.

3.10. Analysis of viability and cell growth

Viable cells were determined by trypan blue (TB) (Sigma Aldrich) exclusion. It was based on the principle that live cells possess intact cell membranes, whereas dead cells do not. Cell suspensions were mixed with TB dye and examined in an optical microscope to determine whether cells take up or exclude dye. The viable cells had a clear cytoplasm whereas the nonviable cells had a blue cytoplasm. Both live and dead cells were counted. From the number of live cells and the respective concentration in culture (live cells/mL) for each day, graphs with culture expansion were drawn taking into account all dilutions made during the follow up. Also, a graph showing the percentage of dead cells in culture per day was designed, through dead cells counting. These graphs were made for each cell line and for each experiment, as seen in *Results* section.

3.11. RNA isolation, primer design and RT-qPCR

After placing in culture BFP positive progenitors collected with FACS sort (Oci-AML3, MOLM13), RNA was extracted from the samples, using TRIzol reagent (ThermoFisher). 200 μL chloroform were used to separate the organic and aqueous phase, by denaturing protein and settling it to the bottom. After collecting of the aqueous phase, 5/6 of this volume of isopropanol (IPA, Honeywell) and 2 μL GenElute TM-LPA (Sigma-Aldrich) were added, respectively to aggregate the RNA to form a pellet and to aid recovery of the RNA during ethanol precipitation with 800 uL EtOH-80%. The extracted RNA was preserved in 20 uL RNasefree Water.

After, it was used to generate first-stand cDNA during reverse transcription. For a single reaction 4 μL 5x VILO^{TM} Reaction Mix and 2 μl 10x SuperScriptTM Enzyme Mix (both Invitrogen) were needed, together with a certain amount of RNA (dependent on qPCR reaction) and DEPC-treated water to get a total volume of 20 μl per reaction.
Primers and probes were used to perform the RT-qPCR (Quantitative reverse transcription polymerase chain reaction).

DNA generated by RT-qPCR was amplified with primers for the different gRNA constructs, which were designed (https://www.ncbi.nlm.nih.gov/tools/primer-blast) to span an exon-exon junction, ideally have a length between 18-22 base pairs and a melting temperature (Tm) of 60°C, and have a PCR product size between 70-150 base pairs. The following primers were used:

		Primers
Human MAT2A	Forward	TGTGCCTGCGAAATACCTTGA
	Reverse	CCCCAACCGCCATAAGTGTC
Mouse mMat2a	Forward	CTGCTTATGCTGCTCGTTGG
	Reverse	AAGAGACCTGAACAAGAACCC

Reverse Transcription-qPCR reactions were performed using Brilliant II SYBR Green qPCR Master Mix (Agilent Technologies) in a CFX96 RealTime System (Bio-Rad). Reactions were set up by making a master mix containing (per reaction): 12.5 uL SYBR Green, 0.125 uL of each Fw and Rv primer and 7.8 uL RNasefree water. To these reactions, 2 uL of DNA template was added. NTC controls without the DNA template were also made. qPCR program settings used were as follows: 50°C for 30 min, 95°C for 10 min, 39× [95°C for 30 s, 60°C for 1 min], 65°C for 30 s and lastly a melting curve with a slow temperature ramp up to 95°C for 30 s.

4. Results

4.1. MAT2A knockout abrogates proliferation of human AML cell lines

I sought to validate the results of the Tzelepis screen through delivery of 5 guide RNAs targeting the MAT2A gene to human AML cell lines with constitutive expression of Cas9. These included the OCI-AML3 and MOLM13 lines in the original screen, as well as Kasumi-1 cells, which had not been previously tested.

In all experiments, triplicate wells were set and infected independently with the go to analyse each of the cell lines in triplicate. However, due to low efficiency of transduction, in most cases sorted cells were pooled and analysed in a single representative experiment, which is reported.

Results present how human AML cell lines, such as Oci-AML3, MOLM13 and Kasumi-1 react to MAT2A knockout (KO). It will validate screen results and understand the mechanism underlying the dependency of MAT2A in AML cell lines.

For this, 5 individual guideRNAs for human gMAT2A were cloned into the lentiviral backbone pKLV2 seen in Figure 11 (see sequences in *Materials and Methods*).

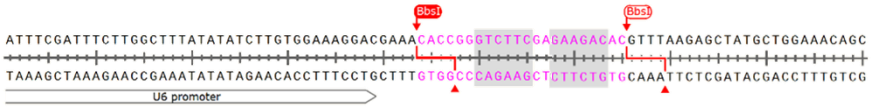

Figure 11 *– Excerpt of pKLV2 plasmid sequence showing BbsI cloning sites either side of the guide RNA scaffold. BbsI digestion generates 2 unique cohesive ends used for insertion of individual gRNAs.*

After the ligation between pKLV2 lentiviral vector and an annealed guide, the sequence that would result is as follows:

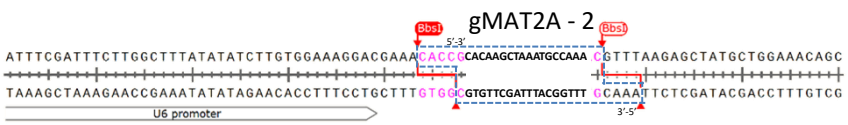

Figure 12 *– Excerpt of pKLV2 plasmid sequence with the 2th guide designed for human MAT2A gene (see sequence in Materials and Methods) incorporated. Guide RNAs are designed as two complementary*

oligonucleotides with unique ends that complement the unique cohesive ends generated through BbsI digestion of pKLV2.

Guide RNA annealing was verified by digestion of recombinant pKLV2 plasmid DNA with *BbsI*. Unlike non-recombinant pKLV2, gRNA incorporation destroys the *BbsI* restriction sites, and no plasmid linearization is produced upon digestion (Figure 13). Candidate recombinant clones were then confirmed by Sanger sequencing. The agarose gel showing the results is underneath:

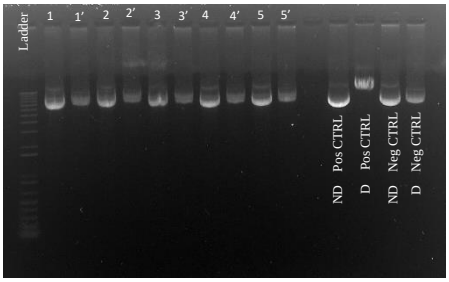

Figure 13 *– Example of a BbsI digestion gel. This gel shows digestion bands of samples with gRNA DNA (non-digested, 1-5 and digested, 1'-5') and the positive and negative controls, represented as non-digested (ND) and digested (D).*

The clones most likely to be recombinant, were sent to sequencing (see one matching sequencing example further ahead in mouse cell lines results) and after confirming the positive ones, I selected one verified clone for each guide and prepared lentiviral particles for guide delivery into human AML cell lines. Cells were transduced with empty (non-recombinant) pKLV2 lentiviral particles, as control. After transduction, cells were sorted on the basis of expression of the Blue Fluorescent Protein (BFP) reporter and their respective cultures monitored for expansion and cell death.

For Oci-AML3 cell line, culture expansion and % of cell death graphs (Figure 14) are shown underneath. We can see that until day 4, Oci-AML3 cells with EV proliferate in a stagnant way. After day 4, EV culture is vividly marked by a growth curve, in which the % of cell death is minimal, reaching only 2,5%. On the other hand, cells transduced with MAT2A guides remain in an almost constant cellular concentration during the follow-up. In cell death graph, achieved through the % of trypan blue posi-

tive cells, we see that MAT2A guide cells had a lower survival rate (75-80%) comparing with EV cells (94-100%).

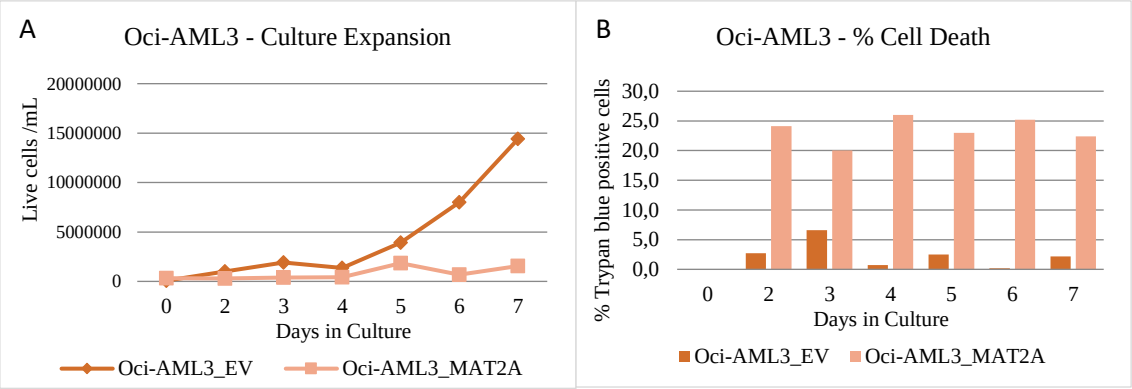

Figure 14 *- A) Live cells /mL and B) % of Cell Death of one performed experiment (n=1). In a general way, Oci-AML3-EV sample proliferates and increases the cell culture. On the other side, MAT2A sample is marked by cell death, with no room to increase cell culture, so that it does not expand like EV sample does.*

For MOLM13 cell line, culture expansion and % of cell death graphs (Figure 15) show that there is a clear difference between expansion of both variants. While EV sample is marked by a three-growing phase proliferation (until day 3 with a lethargic growth, from day 3 until day 5 with a moderately growth and since day 5 with a huge proliferation), cells transduced with MAT2A have half of the cells dying until the last 2 days of the follow-up, decreasing then until a % of death around 25%, once the culture decreases the concentration day by day.

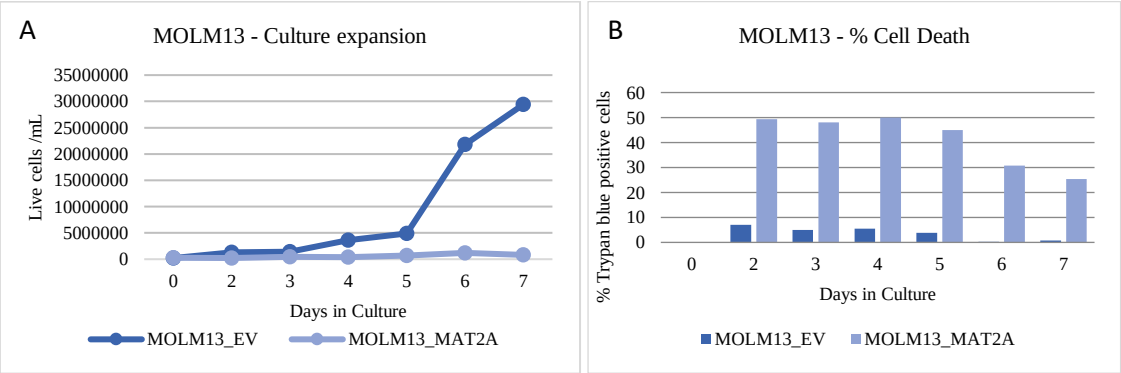

Figure 15 *- A) Live cells /mL and B) % of Cell Death of one performed experiment (n=1). Here, there is no expansion in cell culture of MAT2A sample once the culture growth does not increase and % of cell death is decreasing with the concentration decrement. The opposite is verified in EV sample, inasmuch cell culture is expanding while the % of cell death is decreasing.*

For Kasumi1 cell line, culture expansion and % of cell death graphs (Figure 16) show that Kasumi1 cells with EV guide have a non-homogenic path, though leaving out the day-4 count, once it can be a counting error, cells evidence a good proliferation rate without much percentage of cell death until the last day, marked by a decrease in proliferation, which may be due to the increment of cell death. Meanwhile, cells transduced with MAT2A guides survived well until day-4 even having a constant cell growth line. After that day, proliferation decreased, as well as the survival rate, reaching levels of cell death around 60%.

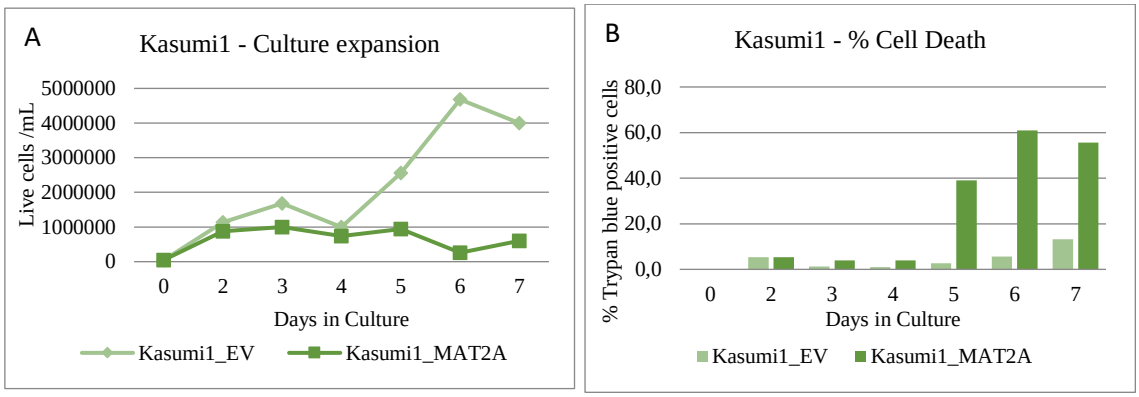

Figure 16 *- A) Live cells /mL and B) % of Cell Death of one performed experiment (n=1). EV sample has a higher culture expansion comparing with MAT2A sample, which is marked by a 50% of cell death in the last days of the followed experiment.*

In general, these graphs show AML cell lines proliferating and growing when they are transduced with empty vectors. By changing transduction to vectors for MAT2A guides, the three different cell lines experience a decrease in proliferation, having constant cell growth paths and a big percentage of death cells, not showing an increment of cell numbers.

I have thus independently confirmed human AML cell line dependency on MAT2A for survival, and extended the results of the Tzelepis screen to Kasumi-1 cells, which represent a distinct common subtype of AML.

I did not initially include the candidate non-responsive MV4.11 cell line (see Figure 6), which would have been important to exclude global toxicity. However, I have investigated mouse primary cell lines carrying corresponding MLL-AF4 and FLT3-ITD (equivalent to non-responsive MV4.11) and MLL-AF9 and FLT3-ITD (equivalent to

MOLM13) to the same end. Nonetheless, meanwhile in the lab, MV4.11 cell line has been studied independently using specific inhibitors.

4.2. Mat2a knockout abrogates proliferation of transformed primary mouse bone marrow cell lines

The same procedures of human AML cell lines were done for primary mouse BM cell lines, MLL-AF4 FLT3^{ITD} and MLL-AF9 FLT3^{ITD}. In this case, 5 individual guideRNAs for mouse gMat2a were cloned into the lentiviral backbone pKLV2, homologously to Figure 11 (see sequences in *Materials and Methods*).

After the ligation between pKLV2 lentiviral vector and the annealed guides as well as the first verification of recombinant pKLV2 plasmid DNA through digestion with *BbsI* and the second verification by sending to sequencing the clones most likely to be recombinant, the data was received and Figure 17 is an example of a matching sequence. In this case it matches with mouse gMat2a-5-Fw (see sequences in *Materials and Methods*). Of note, it would only need one wrong base to be a non-recombinant sequence.

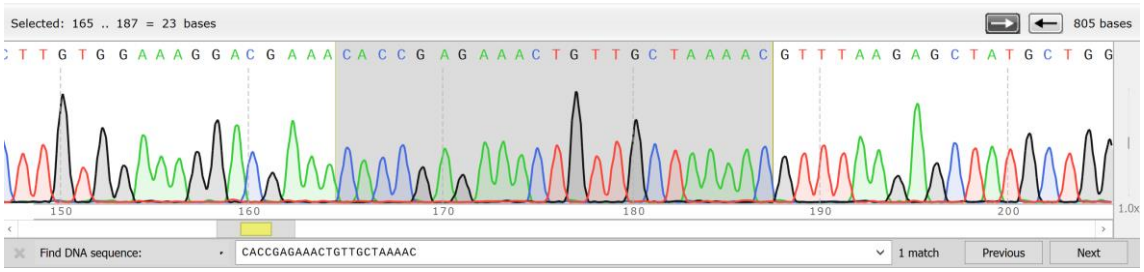

Figure 17 *- Example of a matching sequence of a positive clone with a mouse forward guide (Fw: CACCGAGAAACTGTTGCTAAAAC), done by Source BioScience UK Limited.*

Then, the recombinant clones verified by sequencing results were individually selected to produce lentiviral particles, for later transduction of transformed AML mouse BM cells.

Primary mouse BM cells were transduced as well with empty (non-recombinant) pKLV2 lentiviral particles, as control and after transduction, cells were sorted on the

basis of expression of the Blue Fluorescent Protein (BFP) reporter and their respective cultures monitored for expansion and cell death, like it was done for human cell lines.

For transformed MLL-AF4 FLT3^{ITD} primary mouse BM cells, culture expansion and % of cell death graphs are presented below (Figure 18). MLL-AF4 cells proliferate less comparing with human AML cell lines and after being sorted, EV transduced cells started with a lower number of BFP+ cells than Mat2a ones. During the follow-up, EV sample proliferate, having the biggest rate from day 4 to 6. mMat2a sample decreased cellular concentration in the first 3 days, where since then remained with an approximate similar cellular concentration, once the cells star to die, reaching a cell death percentage of 93%. * Not done.

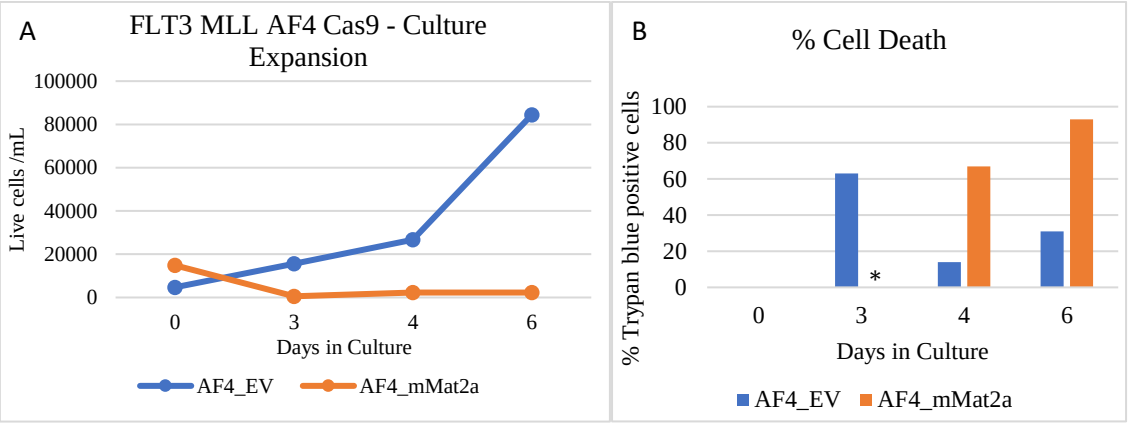

Figure 18 *– A) Live cells /mL and B) % of Cell Death of one performed experiment (n=1). While EV sample recovers and we see a huge proliferation, the same does not happen with the Mat2a sample, in which the % of cell death surpassed the proliferation and so Mat2a sample ends up dying.*

For transformed MLL-AF9 FLT3^{ITD} primary mouse BM cells, proliferation and % of cell death graphs MLL-AF9 show that cells proliferate less comparing with human AML cell lines. Technical replicates which are repeated measurements of the same sample were made three times. The results graph displays the average values and standard deviation (SD) of the mean, which is represented by the error bars. During the follow-up, both samples multiply, having the EV cells the biggest proliferation. As seen in the SD error bars, in the last day of experiment, there is an enormous range of possible results, not allowing a clear analyse. So that, it is difficult to take reliable conclusion. About death rate, we observe that cells transduced with mMat2a-directed guide RNAs

die more comparing with cells with EV. mMat2a sample shows a % of cell death increasing between 37 and 49%, while EV sample increase between 19 and 39%.

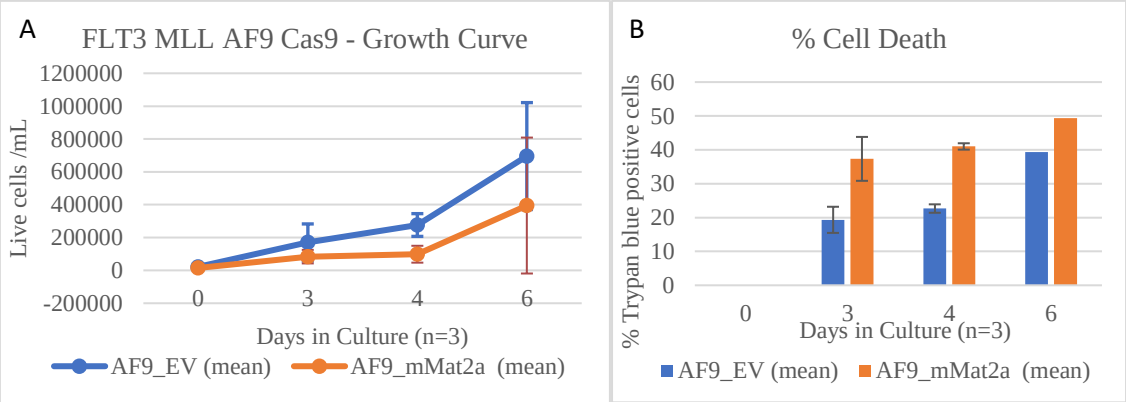

Figure 19 *- A) Live cells /mL and B) % of Cell Death of a performed triplicate experiment (n=3).*

In previous reports, it is known that MLL-AF9 FLT3^{ITD} cells are equivalent to MOLM13 cells in what concerns gene expression profiling (62). Analogously, MLL-AF4 FLT3^{ITD} cells are equivalent to the AML cell line MV4-11 (63), which one was studied in CRISPR screen with results of a non-dependency of MAT2A to survive (22).

Somewhat surprisingly, I observed a dependency of MLL-AF4/FLT3^{ITD}-transformed primary BM cells on Mat2a, while MLL-AF9 FLT3^{ITD} cells were unresponsive to Mat2a depletion. This may reflect differences between mouse and human, and warrant further investigation in additional transformed primary mouse BM clones. Also, it is possible that additional mutations present in the complex karyotype displayed by both MV4.11 and MOLM13 cell lines significantly modify the response to MAT2A loss, in a way that is not captured by the primary mouse lines. Notwithstanding the differences between mouse and human models, the results obtained in mouse confirm cell type-specificity in Mat2a dependency, which is important when considering its therapeutic potential. Once again technical issues prevented replication of the MLL AF4 FLT3^{ITD} experiment which may have an impact on the final results.

4.3. Functional Validation of CRISPR screen

In order to validate dependency of AML cells lines on MAT2A expression by an independent means, I designed multiple shRNAs (See Materials and Methods) targeting the MAT2A coding sequence in order to achieve MAT2A knockdown by RNA interference. Those were cloned into the lentiviral vector pLL3.7 and to fulfil the cloning procedure, pLL3.7 was digested with *XhoI* and *HpaI* restrict enzymes and the linearized DNA vector was cut out from the gel and further purified (QIAquick Gel Extraction Kit, QUIAGEN) as follows:

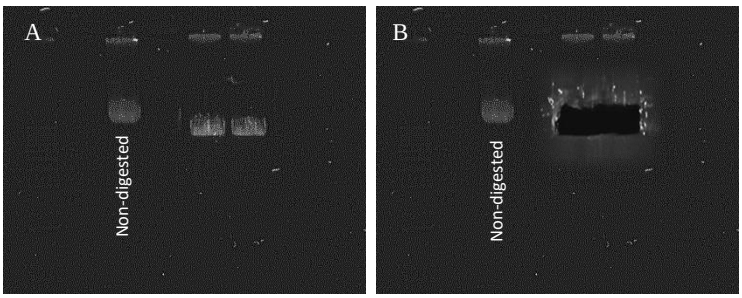

Figure 20 *- Digestion gels. A) showing the negative control non-digested and both wells with digested product. B) showing the cut out of plasmid DNA to former use gel extraction kit.*

After cloning procedure (see *Materials and Methods*) was the sequence validation step, to make sure we had the shMAT2A incorporated inside pLL3.7. A PCR screening and a *BamHI* digestion were performed to select the most likely positive clones and then send them for sequencing. The results are as follows:

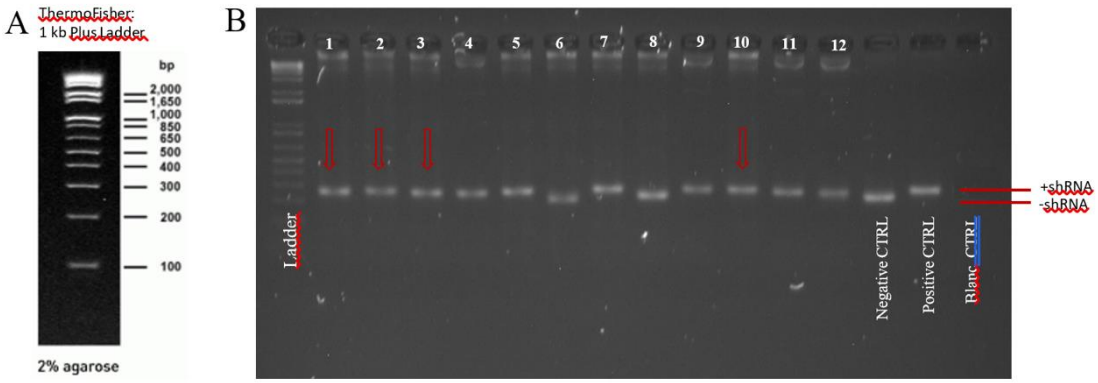

Figure 21 *– A) 1 Kb Plus DNA ladder for a 2% agarose gel with quantity of base pairs per bar represented. B) Gel of DNA multiplied by PCR screen, run on a 2% agarose gel. First loading well contained the 1 Kb plus DNA ladder, followed by 12 samples. Three controls followed next: negative and positive*

controls to be able to detect positive clones, and a blanc control to check for contamination. Positive samples, which are the ones with the shRNA inserted, are represented in the same line of the positive control, a little higher than the negative samples. These last ones, as we can see clearly in the samples 6 and 8, do not have the shRNA inserted, since the used primers cannot amplify the inserted shRNA region. Red arrows indicate positive clones, which were sent for sequencing. This gel shows bands of shMAT2A_1 (1-8) and shMAT2A_2 (9-12) DNA.

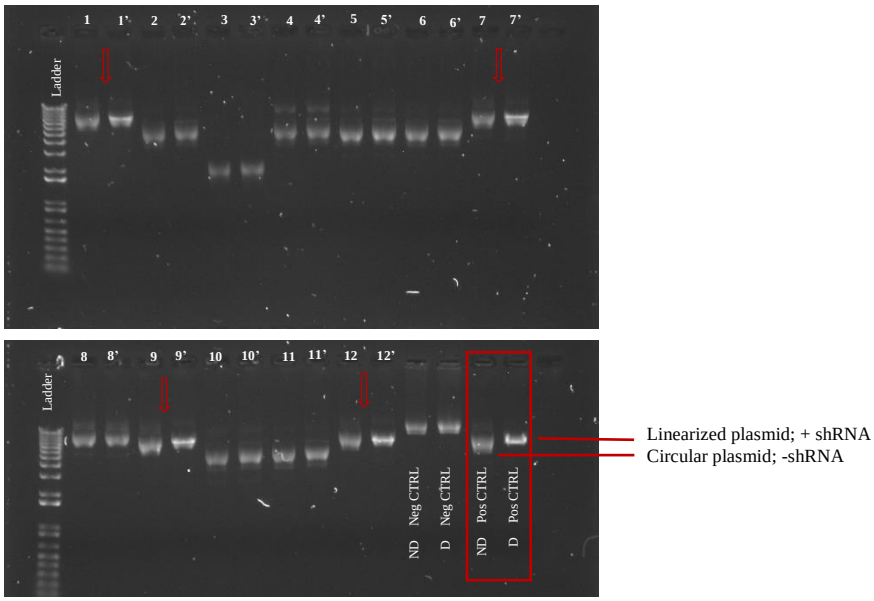

Figure 22 *- BamHI digestion for screen for positive clones, run on a 0.8% agarose gel. First loading well, in both gels, contained the 1 Kb plus DNA ladder, followed by the samples, in which the numbers (1) represent undigested plasmid and the numbers followed by the sign ' (1'), represent the digested vector. Positive and negative controls run in the gel 2, in the last 4 wells. Positive clones had the same appearance as the positive control. When digested, the positive clones appear as linearized plasmid, while the non-digested appears as a circular plasmid. Red arrows indicate positive clones, which were sent for sequencing. This gel shows the difference of digested (1-12) and non-digested (1'-12') samples of shMAT2A_2.*

Then, the most possible positive clones were sent for sequencing and the following figure exemplifies a positive result, where it is possible to verify the sequence of shMAT2A.

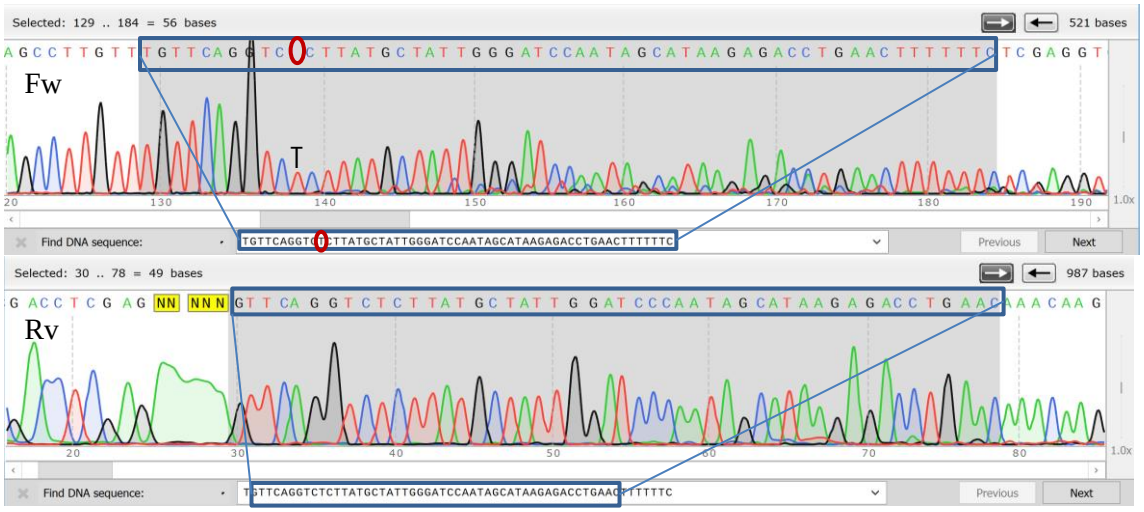

Figure 23 *- Example of matching sequences of a positive clone with shMAT2A, Fw and Rv (shMAT2A-2 Fw:TGTTCAGGTCTCTTATGCTATTGGGATCCAATAGCATAAGAGACCTGAACTTTTTTC), done by Source BioScience UK Limited.*

Being sure about the positive clone, lentiviral particles were produced to infect Oci-AML3 cell line. Right after, the transduced cells were sorted for GFP+ positive cells and cultured for testing of MAT2A knockdown and evaluation of the effects of MAT2A reduction on growth and death of transduced OCI-AML3 cells.

4.3.1.Validation of Knockdown

To validate the knockdown (KD) of MAT2A, another RT-qPCR were performed by Pina's lab group with Oci-AML3. Like previously, ACTB and GAPDH were both used as controls. Besides, two technical replicates were made, so that a standard deviation is represented by error lines. Result of KD in Oci-AML3 cells is as follows:

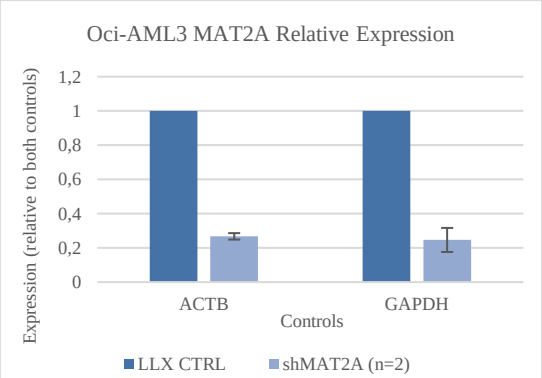

Figure 24 *- MAT2A expression relative to ACTB and GAPDH controls, individually. Relative to both controls, the expression level of MAT2A gene dropped to 27 and 25%, respectively. Standard Deviation error bars indicate that KD relative to ACTB has an error of 2% and relative to GAPDH the error can go up until 7%.*

The graph shows a marked decrease in the expression of MAT2A gene, represented by the orange bars, for both controls, with a level of knockdown of just under 75%. Thus, with this functional validation of knockdown we confirm the true dependency of MAT2A for cells development.

Similar to my observations in the MAT2A-directed CRISPR experiments, I observed decreased growth and enhanced cell death in the knockdown cultures. Specifically, growth curves and cell death were followed-up for 6 days after GFP+ sort collection and two technical replicates were made. Also, cells were counted with Trypan Blue method, described in *Materials and Methods*. Cell profile graphs are underneath (Figure 25). From day 1 to day 3, live cells path seems similar inside each variant individually: LLX CTRL samples increase proliferation while in shMAT2A samples, we do not observe cell expansion. Until day 6 LLX CTRL cells start to proliferate in a more advanced rate, comparing with shMAT2A condition in which one sample (shMAT2A-1) remains in almost constant cellular concentration and the other sample (shMAT2A-2) end up dying. In cell death graph, achieved through the % of trypan blue positive cells, we see that after the first day, all cells recover, decreasing the % of cell death. By day 6, LLX CTRL-1 decrease to 80% cell survival and LLX CTRL-2 recover, presenting 100% of survival, while shMAT2A-2, as described before, ends up dying and shMAT2A-1 increase survival rate up to 80%, from 60% at first day.

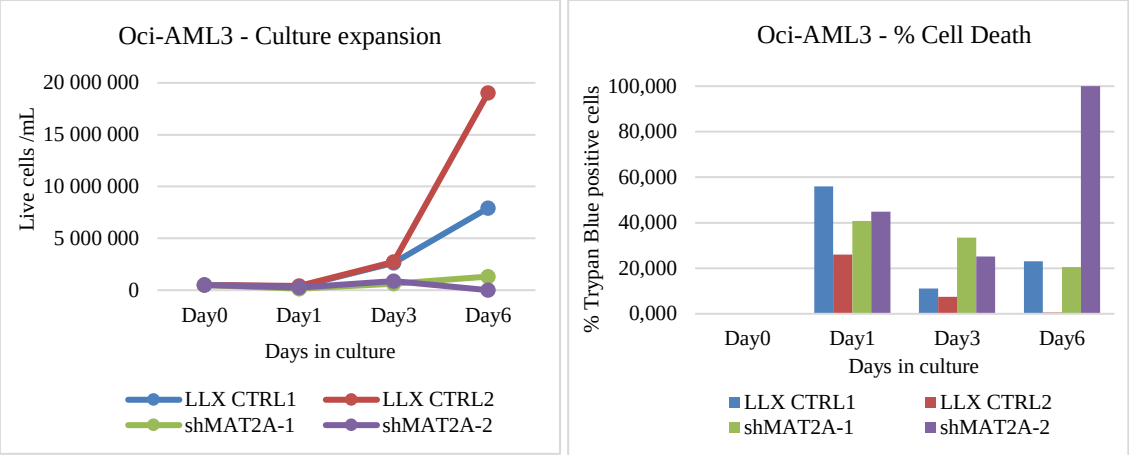

Figure 25 *– A) Live cells /mL and B) % of Cell Death of a performed duplicate experiment (n=2). In general, LLX CTRL samples increase proliferation, reducing cell death. Meanwhile, in shMAT2A cells, we do not observe cell culture expansion, and cell death path is not regular, decreasing day-by-day in one sample (shMAT2A-1) and decreasing first until day 3 but ending up dying in the last day in the other sample (shMAT2A-2), with a 100% of cell death.*

Looking over the graphs, we see that cells transduced with shCTRL have a higher expansion during the 6 days, especially after day-3, comparing with cells with shMAT2A. At the same time, % of dead cells shows a considerable death rate in the first day, with an average of 43% for shMAT2A and 41% for LLX CTRL. From the first day seems like the cells recovered until day 3, in the sense of dying less or proliferating more.

Linking both graphs, it is correct to affirm that shMAT2A cells did not proliferate as the CTRLs (Figure 25 – Culture expansion) because they were dying more (Figure 25 – Cell death). Accordingly, and once again, we show that MAT2A gene can be related with the survival and proliferation of Leukemic cells, once we demonstrated a KD on MAT2A gene and a decreasing in proliferation rate (or cellular survival) in Oci-AML3 shMAT2A samples. This achievement can come up with a new way of treatment AML disease in future.

4.4. Confirming direct validation of CRISPR screen

I attempted to confirm gene expression knockout of MAT2A by quantitative RT-PCR analysis of Cas9-expressing OCI-AML3 and MOLM13 cell lines transduced with a pool of MAT2A-directed guide RNAs. I extracted RNA and synthesised cDNA from transduced cells cultured for 7 days in the presence of the guides. I used 2 pairs of primers directed to MAT2A coding sequence located upstream and downstream of the region targeted by the guide RNAs. Figure 26 shows the coding sequence (CDS) of MAT2A mRNA, highlighting the primers, the 5 guides for human MAT2A gene and the tip and tail of each exon.

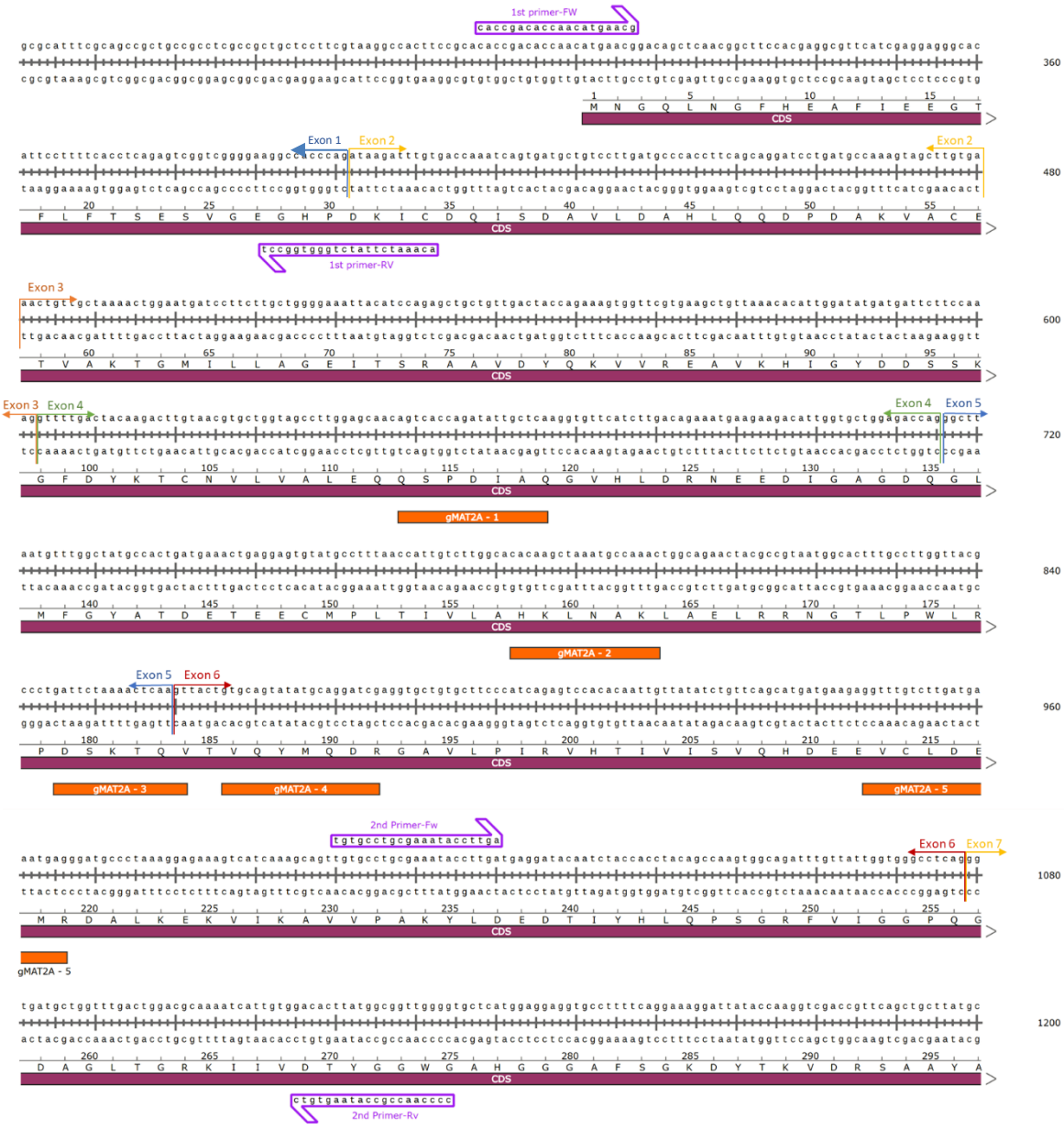

Figure 26 – *CDS sequence of MAT2A gene. Guides location are represented in orange rectangles. Primer sets are highlighted with a purple arrow and the tip and toes of the exons are also represented with different colour arrows for each exon. Figure was designed with SnapGene Viewer 3.3.3. Gene mRNA sequence was taken out from* (64)

Both pairs of primers were designed across exon boundaries, and generated a single amplicon in control and targeted samples, compatible with amplification of cDNA, but not genomic DNA. Figures 27 shows the dissociation curve of the primer set spanning exons 1 and 2, where we can validate the single amplicon generated in PCR.

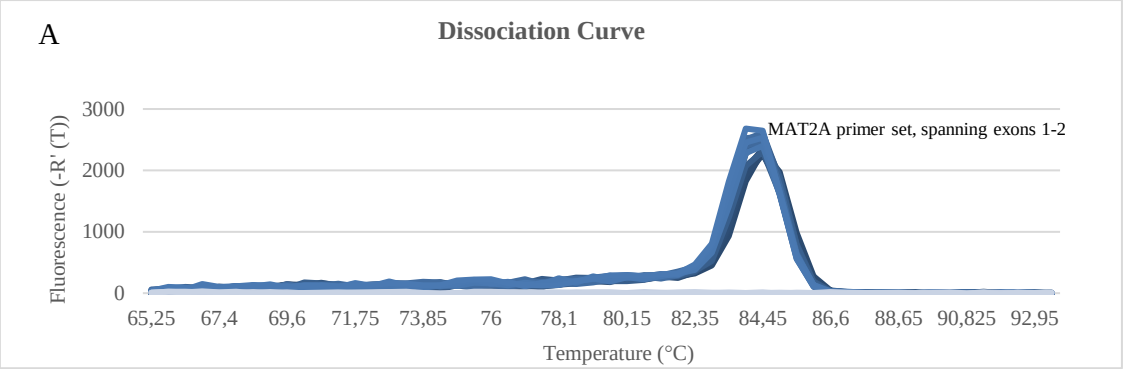

Figure 27 *– A) Dissociation curve of the qPCR test with annealing temperature set at 65,25 °C showing high peak at ± 84,5 ºC of four populations in a n=3 experiment: MOLM13-EV, MOLM13-MAT2A, Oci-AML3-EV and Oci-AML3-MAT2A, which correspond to MAT2A primer set that span the exons 1 and 2.*

I did not observe reduction or loss of MAT2A transcript in none of cell lines using both primer sets (Figures 28A and 28B), which is surprising for the downstream one, as at least a proportion of the NHEJ events subsequent to Cas9-mediated endonuclease activity were likely to have introduced premature stop codons and reduced subsequent downstream transcription. Alternatively, the generation of a proportion of frameshift mutations would have resulted in targeting of RNA to non-sense RNA decay mechanisms, also leading to reduction in transcript levels. I did not have enough material to verify the levels of knockout at the level of protein production by Western blot, which would be the next logical experiment.

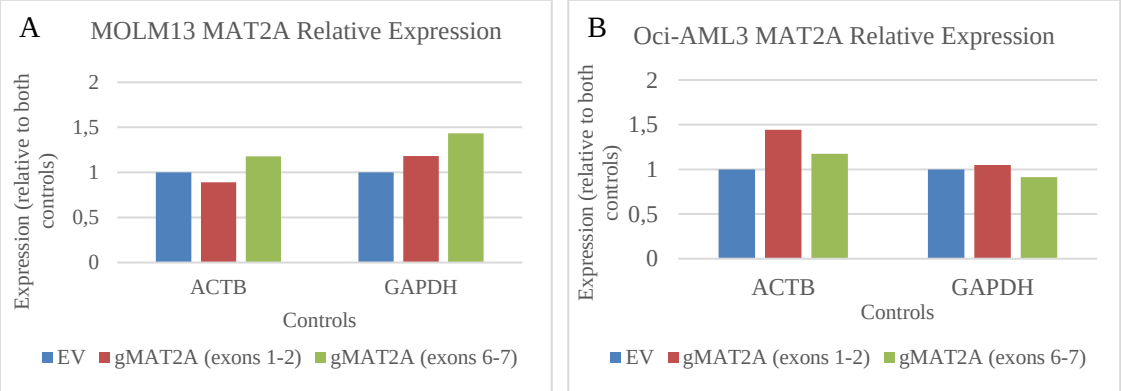

Figure 28 *– MAT2A expression relative to ACTB and GAPDH controls, individually, regarding both MAT2A primer sets. Red columns correspond to RT-qPCR using MAT2A primers spanning exons 1 and 2 of gMAT2A samples, while green columns are related with MAT2A primers that span exons 6 and 7. Considering all conditions, no considerable loss of MAT2A gene expression is observed. A) Related with MOLM13 cell line. B) Related with Oci-AML3 cell line.*

Assuming absence of detectable knockout in cultured cells expressing the BFP+ guide RNA construct, one possible explanation is that the surviving cells in the culture failed to express the guide RNA, which is transcribed from a RNA Pol U6 promoter distinct from the RNA PGK promoter driving expression or BFP. More likely, the surviving cells may not exhibit Cas9 activity, despite expression of the construct in the culture, as these were not clonally-derived. Tzelepis *et al.* effectively showed that 50% of clones did not show Cas9 activity. Another hypothesis is that these clones have taken over the culture upon death of the MAT2A knockout cells (22). Although this is an interesting point to clarify in future experiments, the validation of the CRISPR/Cas9 results by shRNA-mediated knockdown of MAT2A expression, and more recently, by MAT2A chemical inhibition (performed independently from this work in the PINA lab), support a dependency of AML cultured lines on MAT2A, which may be of therapeutic relevance.

5. Conclusions and Future Perspectives

According to a CRISPR Dropout Screen (22) developed in order to understand the genetic vulnerabilities of cancer cells, 492 genes were found as AML-specific cell-essential genes, which can be perceived as new targets for therapeutic strategies. From that research, the study of molecular mechanisms underlying tumorigenesis were thought-about as well. Among those genes, MAT2A was found to be essential for AML cell lines survival. The work presented in this thesis led to an initial validation of that CRISPR screen by independent gRNA cloning and testing in Cas9 expressing cells and broaden it into an additional cell line, of those ones cover in the paper. To clarify, MOLM13 and Oci-AML3 cell lines were shown to depend on MAT2A, according to the conclusions of CRISPR screen and Kasumi1 cell line allowed the extension of CRISPR results. In the three cell lines we validate the dependency of MAT2A once, by comparing with the empty vector control, cells transduced with guides for MAT2A decreased their proliferation and their survival rate.

Furthermore, this work also allowed the development of tools for investigation of CRISPR-mediated knockout of Mat2a in mouse cells. Two different mouse model cell lines were searched as well, contributing to the enlargement of CRISPR results. Transformed MLL-AF4 $FLT3^{ITD}$ and MLL-AF9 $FLT3^{ITD}$ primary mouse bone marrow cells were tested for the dependency of Mat2a gene.

Moreover, design, cloning and validation of MAT2AshRNA constructs for gene expression knockdown in human cells were tested and it made possible the creation of important tools, once shRNA knockdown is currently more easily amenable to use in primary patient AML cells.

During the development of the following thesis, general caveats of data should have been taken into consideration and this awareness can be useful in future experiments.

As explained in the result section, technical difficulties throughout replication of the number of the experiments was confronted so that the designed experiments were not possible to perform and a fool validation of the results require it to make every result more reliable and to take more consistent conclusions.

Also, experimental setbacks left us with no live cells remaining of Kasumi1, MLL-AF4 and MLL-AF9, so that they were not submitted to the RT-QPCR.

Our gene of interest, MAT2A, encodes a specific isoform of MAT gene, which is a key enzyme in metabolism, because it catalyses the synthesis of S-adenosylmethionine (SAM), the major methyl group donor. The process in which SAM is originated needs methionine and it is thought that cancer cells can be methionine dependent in what concerning the lack of SAM. The reason cancer cells depend on high levels of SAM remains to be discover. Further experiments related with the measurement of SAM levels produced in cells would be interesting. The relation between inhibition of MAT2A and the remaining capacity of cells to produce SAM can be a grant to study the capacity of cells to proliferate in a non-regular way. Relating this discovers with published data, it is demonstrated that only cancer cells are affected by methionine deficiency (45), which can make us consider about the therapeutic effects of MAT2A loss in AML cells. But it leads us to another research that must be made before taking any conclusions about the transversely of solid cancer cells and blood leukemic cells. Nevertheless, the results described here need to be tested once again in normal cells, *i.e* results must be evaluated as a function of the dependence of MAT2A on normal cells, in order to be a valid therapeutic which affects only AML cells.

In this thesis we inhibited our gene of interest and we relied in the absence of the gene in the results. However, there are two products that can be altered when there is a gene inhibition: DNA and proteins. Here we only examined DNA expression, without checking at the protein level. The option of having expression of cDNA but no proteins can happen. As said before, it remains possible to have an in-frame repair with the production of a transcribed mRNA molecule or it could have a dissociation in gRNA and BFP expression which have might led to only BFP selection leaving aside MAT2A guides. In a future experiment, a validation of gene expression loss at the protein level by western-blot can be performed to detect specific MAT2A proteins using antibodies, instead of searching for cDNA expression.

Nowadays despite traditional treatments for Acute Myeloid Leukemia, 10,590 people are expected to die from this malignancy in 2017 and an estimated 21,380 new cases are expected in the current year (65). Research and discover new treatments are urgent. Besides, understanding the pathogenesis at a genomic and molecular level has

often come to light in different researches (66). New treatments can be developed by identifying cancerous cells vulnerabilities. The overall purpose of this thesis was to describe the study of one possible novel treatment, related with gene editing, lightening away the traditional options to overcome leukemias.

Another huge contribution to the study of different and new options to cure leukemia is to delineate experiments to measure the metabolic and transcriptional consequences of depleting MAT2A.

Moreover, one interesting approach related with pharmaceutical industry is related with SAM inhibitors. It was discovered some years ago a molecule that is cable of inhibiting MAT2A gene in primary cells. The cell-permeable fluorinated N,N-dialkylaminostilbene (FIDAS) inhibits MAT2A-catalyzed SAM (S-adenosylmethionine) synthesis by targeting SAM-binding pocket at the MAT2A dimer interface. There are two different classes of FIDAS: -3 and -5, which the last one is more than 2 times more potent than FIDAS-3 in inhibiting MAT2A-catalyzed SAM synthesis. They were shown to downregulate intracellular SAM level (by 60%; 36 h) with 10 μM of FIDAS-3 and 3 μM of FIDAS-5 (67). With this possibility it could be interesting to study the role of FIDAS in AML cell lines at the same time as a validation of this work inhibiting MAT2A by gene editing. Moreover, they could be used to support the data obtained, and to extend the investigation to patient cells *in vitro* and *in vivo*.

Finally, this project led me to deeply understand the molecular basis of one carbon cycle and the cell machinery involved in methylation steps. It enabled the validation of the results concerning the loss of a vulnerable gene previously shown by Tzelepis *et al*. (22), allowing opening the door to innovative new treatments for leukemia. The present work is part of a vast effort to understand the new therapeutic paths that will be tackled in the near future to overcome leukemias.

6. References

1. Alessandrini M, Kappala SS, Pepper MS. AMLprofiler: A Diagnostic and Prognostic Microarray for Acute Myeloid Leukemia. 2017;1633:101–23.

2. CancerResearchUK. Acute myeloid leukaemia (AML) incidence statistics [Internet]. [cited 2017 Oct 26]. Available from: http://www.cancerresearchuk.org/health-professional/cancer-statistics/statistics-by-cancer-type/leukaemia-aml

3. Gilliland DG. The Molecular Basis of Leukemia. Hematology [Internet]. 2004;2004(1):80–97. Available from: http://asheducationbook.hematologylibrary.org/content/2004/1/80.full

4. Coalson DW, Mecham J, Stern PH, Hoffman RM. Reduced availability of endogenously synthesized methionine for S-adenosylmethionine formation in methionine-dependent cancer cells. 1982;79(July):4248–51.

5. Acute Myeloid Leukemia Staging [Internet]. [cited 2017 Oct 12]. Available from: http://emedicine.medscape.com/article/2006750-overview

6. Kumar CC. Genetic Abnormalities and Challenges in the Treatment of Acute Myeloid Leukemia. Genes Cancer [Internet]. 2011;2(2):95–107. Available from: http://gan.sagepub.com/lookup/doi/10.1177/1947601911408076

7. Ratcliffe MJH. Encyclopedia of Immunobiology [Internet]. Elsevier Science; 2016. Available from: https://books.google.pt/books?id=Q53vAwAAQBAJ

8. Martens JHA, Stunnenberg HG. The molecular signature of oncofusion proteins in acute myeloid leukemia. FEBS Lett. 2010;584(12):2662–9.

9. Mueller BU, Pabst T, Fos J, Petkovic V, Fey MF, Asou N, et al. ATRA resolves the differentiation block in t(15;17) acute myeloid leukemia by restoring PU.1 expression. Vol. 107, Blood. 2006. p. 3330–8.

10. Jing Y. The PML-RARalpha fusion protein and targeted therapy for acute promyelocytic leukemia. Leuk Lymphoma [Internet]. 2004;45(4):639–48. Available from: http://www.ncbi.nlm.nih.gov/pubmed/15160934

11. Vangala RK, Heiss-Neumann MS, Rangatia JS, Singh SM, Schoch C, Tenen DG, et al. The myeloid master regulator transcription factor PU.1 is inactivated by AML1-ETO in t(8;21) myeloid leukemia. Blood. 2003;101(1):270–7.

12. Pabst T, Mueller BU, Harakawa N, Schoch C, Haferlach T, Behre G, et al. AML1-ETO downregulates the granulocytic differentiation factor C/EBPalpha in t(8;21) myeloid leukemia. Nat Med. 2001;7(4):444–51.

13. Moreno-Miralles I, Pan L, Keates-Baleeiro J, Durst-Goodwin K, Yang C, Kim HG, et al. The inv(16) cooperates with ARF haploinsufficiency to induce acute myeloid leukemia. J Biol Chem. 2005;280(48):40097–103.

14. Krivtsov A V., Armstrong SA. MLL translocations, histone modifications and leukaemia stem-cell development. Nat Rev Cancer [Internet]. 2007;7(11):823–33. Available from: http://www.nature.com/doifinder/10.1038/nrc2253

15. Hoffbrand AV, Moss PAH. Essential Haematology. Wiley; 2001. (Essentials).

16. Falini B, Nicoletti I, Bolli N, Martelli MP, Liso A, Gorello P, et al. Translocations and mutations involving the nucleophosmin (NPM1) gene in lymphomas and leukemias. Haematologica. 2007;92(4):519–32.

17. Liu Y, He P, Liu F, Shi L, Zhu H, Zhao J, et al. Prognostic significance of NPM1 mutations in acute myeloid leukemia: A meta-analysis. Mol Clin Oncol [Internet]. 2014 Mar 10;2(2):275–81. Available from: http://www.ncbi.nlm.nih.gov/pmc/articles/PMC3917771/

18. Gary Gilliland D, Griffin JD. The roles of FLT3 in hematopoiesis and leukemia. Blood. 2002;100(5):1532–42.

19. Blau O. Gene Mutations in Acute Myeloid Leukemia — Incidence , Prognostic Influence , and Association with Other Molecular Markers. InTechOpen [Internet]. 2015; Available from: https://www.intechopen.com/books/leukemias-updates-and-new-insights/gene-mutations-in-acute-myeloid-leukemia-incidence-prognostic-influence-and-association-with-other-m

20. Lee BH, Tothova Z, Levine RL, Anderson K, Buza-Vidas N, Cullen DE, et al. FLT3 Mutations Confer Enhanced Proliferation and Survival Properties to Multipotent Progenitors in a Murine Model of Chronic Myelomonocytic Leukemia. Cancer Cell. 2007;12(4):367–80.

21. Levis M, Small D. FLT3: ITDoes matter in leukemia. Leuk Off J Leuk Soc Am Leuk Res Fund, UK. 2003;17(9):1738–52.

22. Tzelepis K, Koike-yusa H, Braekeleer E De, Pina C, Vassiliou GS, Yusa K, et al. A CRISPR Dropout Screen Identifies Genetic Vulnerabilities and Therapeutic Targets in Acute Resource A CRISPR Dropout Screen Identifies Genetic Vulnerabilities and Therapeutic Targets in Acute Myeloid Leukemia. 2016;1193–205.

23. Bowen DT, Frew ME, Hills R, Gale RE, Wheatley K, Groves MJ, et al. RAS mutation in acute myeloid leukemia is associated with distinct cytogenetic subgroups but does not influence outcome in patients younger than 60 years. Blood [Internet]. 2005;106(6):2113–9. Available from: http://bloodjournal.hematologylibrary.org/content/106/6/2113.short

24. Wang J, Liu Y, Li Z, Wang Z, Tan LX, Ryu M-J, et al. Endogenous oncogenic Nras mutation initiates hematopoietic malignancies in a dose- and cell type-dependent manner. Blood [Internet]. 2011 Jul 14;118(2):368–79. Available from: http://www.ncbi.nlm.nih.gov/pmc/articles/PMC3138689/

25. COSMIC - Catalogue of Somatic Mutations in Cancer - DNMT3A [Internet]. [cited 2017 Oct 16]. Available from: http://cancer.sanger.ac.uk/cosmic/gene/analysis?ln=DNMT3A#references

26. Tiacci E, Spanhol-Rosseto A, Martelli MP, Pasqualucci L, Quentmeier H, Grossmann V, et al. The NPM1 wild-type OCI-AML2 and the NPM1-mutated OCI-AML3 cell lines carry DNMT3A mutations. Leukemia [Internet]. 2012;26(3):554–7. Available from: http://www.nature.com/leu/journal/v26/n3/pdf/leu2011238a.pdf

27. Shih AH, Abdel-Wahab O, Patel JP, Levine RL. The role of mutations in epigenetic regulators in myeloid malignancies. Immunol Rev [Internet]. 2015;263(1):22–35. Available from: http://dx.doi.org/10.1038/nrc3343

28. Reindl C, Quentmeier H, Petropoulos K, Greif PA, Benthaus T, Argiropoulos B, et al.

CBL exon 8/9 mutants activate the FLT3 pathway and cluster in core binding factor/11q deletion acute myeloidLeukemia/myelodysplastic syndrome subtypes. Clin Cancer Res. 2009;15(7):2238–47.

29. Schnittger S, Bacher U, Alpermann T, Reiter A, Ulke M, Dicker F, et al. Use of CBL exon 8 and 9 mutations in diagnosis of myeloproliferative neoplasms and myelodysplastic/myeloproliferative disorders: An analysis of 636 cases. Haematologica. 2012;97(12):1890–4.

30. Barrangou R, Fremaux C, Deveau H, Richards M, Boyaval P, Moineau S, et al. CRISPR Provides Acquired Resistance Against Viruses in Prokaryotes. Science (80-) [Internet]. 2007;315(5819):1709–12. Available from: http://www.sciencemag.org/cgi/doi/10.1126/science.1138140

31. Wang T, Wei JJ, Sabatini DM, Lander ES. Genetic Screens in Human Cells Using the CRISPR-Cas9 System. Science (80-) [Internet]. 2014;343(6166):80–4. Available from: http://www.sciencemag.org/lookup/doi/10.1126/science.1246981

32. CRISPR & TALEN Genome Editing Tools [Internet]. [cited 2017 Oct 10]. Available from: http://www.genecopoeia.com/product/genome-editing-tools/genome-editing/

33. Moore CB, Guthrie EH, Huang MT, Taxman DJ. Short Hairpin RNA (shRNA): Design, Delivery, and Assessment of Gene Knockdown. 2010;629(2):1–15. Available from: http://link.springer.com/10.1007/978-1-60761-657-3

34. Sims D, Mendes-Pereira AM, Frankum J, Burgess D, Cerone M-A, Lombardelli C, et al. High-throughput RNA interference screening using pooled shRNA libraries and next generation sequencing. Genome Biol [Internet]. 2011;12(10):R104. Available from: http://genomebiology.biomedcentral.com/articles/10.1186/gb-2011-12-10-r104

35. Evers B, Jastrzebski K, Heijmans JPM, Grernrum W, Beijersbergen RL, Bernards R. CRISPR knockout screening outperforms shRNA and CRISPRi in identifying essential genes. Nat Biotechnol [Internet]. 2016;34(6):631–3. Available from: http://www.nature.com/doifinder/10.1038/nbt.3536

36. Bhinder B, Shum D, Djaballah H. Comparative analysis of RNAi screening technologies at genome-scale reveals an inherent processing inefficiency of the plasmid-based shRNA hairpin. Comb Chem High Throughput Screen [Internet]. 2014;17(2):98–113. Available from: http://www.ncbi.nlm.nih.gov/pmc/articles/PMC4007059/

37. Cojocari D. Lentiviral delivery of shRNA and the mechanism of RNA interference in mammalian cells. University of Toronto; 2010.

38. Bolander-Gouaille C, Bottiglieri T. Homocysteine : Related Vitamins and Neuropsychiatric Disorders. 2nd ed. Editions S, editor. Paris France; 2007. 217 p.

39. Mentch SJ, Locasale JW. One-carbon metabolism and epigenetics : understanding the specificity. 2015;91–8.

40. Cavuoto P, Fenech MF. A review of methionine dependency and the role of methionine restriction in cancer growth control and life-span extension. Cancer Treat Rev [Internet]. 2012;38(6):726–36. Available from: http://dx.doi.org/10.1016/j.ctrv.2012.01.004

41. Anderson ME. Glutathione: An overview of biosynthesis and modulation. Chem Biol Interact. 1998;111–112:1–14.

42. Hitchler MJ, Domann FE. An epigenetic perspective on the free radical theory of

development. Free Radic Biol Med. 2007;43(7):1023–36.

43. Sugimura T, Birnbaum SM, Winitz M, Greenstein JP. Quantitative nutritional studies with water-soluble, chemically defined diets. VIII. The forced feeding of diets each lacking in one essential amino acid. Arch Biochem Biophys [Internet]. 1959;81(2):448–55. Available from: http://ac.els-cdn.com/0003986159902255/1-s2.0-0003986159902255-main.pdf?_tid=621c38fc-145b-11e5-934a-00000aab0f27&acdnat=1434482022_a770b03b1fb8ca20f7d2f3f24181bb30

44. Kokkinakis DM, Liu X, Chada S, Ahmed MM, Shareef MM, Singha UK, et al. Modulation of gene expression in human central nervous system tumors under methionine deprivation-induced stress. Cancer Res [Internet]. 2004;64(20):7513–25. Available from: http://www.ncbi.nlm.nih.gov/entrez/query.fcgi?cmd=Retrieve&db=PubMed&dopt=Citation&list_uids=15492278

45. Cellarier E, Durando X, Vasson MP, Farges MC, Demiden A, Maurizis JC, et al. Methionine dependency and cancer treatment. Cancer Treat Rev. 2003;29(6):489–99.

46. Breillout F, Antoine E, Poupon MF. Methionine Dependency of Malignant Tumors: A Possible Approach for Therapy. JNCI J Natl Cancer Inst [Internet]. 1990;82(20):1628–32. Available from: +

47. Booher K, Lin DW, Borrego SL, Kaiser P. Downregulation of Cdc6 and pre-replication complexes in response to methionine stress in breast cancer cells. Cell Cycle. 2012;11(23):4414–23.

48. Shafqat N, Muniz JRC, Pilka ES, Paragrigoriou E, von Delft F, Oppermann U, et al. Insight into S-adenosylmethionine biosynthesis from the crystal structures of the human methionine adenosyltransferase catalytic and regulatory subunits. Biochem J [Internet]. 2013;452(1):27–36. Available from: http://biochemj.org/lookup/doi/10.1042/BJ20121580%5Cnhttp://www.pubmedcentral.nih.gov/articlerender.fcgi?artid=3793261&tool=pmcentrez&rendertype=abstract%5Cnhttp://www.ncbi.nlm.nih.gov/pubmed/23425511

49. Firestone RS, Schramm VL. “Transition-State Structure for Human MAT2A from Isotope Effects.” J Am Chem Soc [Internet]. 2017;jacs.7b05803. Available from: http://pubs.acs.org/doi/abs/10.1021/jacs.7b05803

50. Cai J, Mao Z, Hwang JJ, Lu SC. Differential expression of methionine adenosyltransferase genes influences the rate of growth of human hepatocellular carcinoma cells. Cancer Res. 1998;58(7):1444–50.

51. Sánchez Del Pino MM, Pérez-Mato I, Sanz JM, Mato JM, Corrales FJ. Folding of dimeric methionine adenosyltransferase III: Identification of two folding intermediates. J Biol Chem. 2002;277(14):12061–6.

52. Wang Q, Liu Q, Liu Z-S, Qian Q, Sun Q, Pan D. Inhibition of hepatocelluar carcinoma MAT2A and MAT2beta gene expressions by single and dual small interfering RNA. J Exp Clin Cancer Res [Internet]. 2008;27:72. Available from: http://www.pubmedcentral.nih.gov/articlerender.fcgi?artid=2613873&tool=pmcentrez&rendertype=abstract

53. Liu Q, Wu K, Zhu Y, He Y, Wu J, Liu Z. Silencing MAT2A gene by RNA interference inhibited cell growth and induced apoptosis in human hepatoma cells. Hepatol Res. 2007;37(5):376–88.

54. Chen H, Xia M, Lin M, Yang H, Kuhlenkamp J, Li T, et al. Role of Methionine Adenosyltransferase 2A and S-adenosylmethionine in Mitogen-Induced Growth of Human Colon Cancer Cells. Gastroenterology. 2007;133(1):207–18.

55. Phuong NTT, Kim SK, Im JH, Yang JW, Choi MC, Lim SC, et al. Induction of methionine adenosyltransferase 2A in tamoxifen-resistant breast cancer cells. Oncotarget. 2016;7(12):13902–16.

56. Dawson MA, Prinjha RK, Dittmann A, Giotopoulos G, Bantscheff M, Chan W, et al. Inhibition of BET recruitment to chromatin as an effective treatment for MLL-fusion leukaemia. Nature [Internet]. 2011;478(7370):529–33. Available from: http://dx.doi.org/10.1038/nature10509

57. Montes R, Gutierrez-aranda I, Prat I, Herna MC, Ponce L, Bresolin S, et al. Enforced expression of MLL-AF4 fusion in cord blood CD34 ♀ cells enhances the hematopoietic repopulating cell function and clonogenic potential but is not sufficient to initiate leukemia. 2017;117(18):4746–59.

58. Quentmeier H, Martelli MP, Dirks WG, Bolli N, Liso a, Macleod R a F, et al. Cell line OCI/AML3 bears exon-12 NPM gene mutation-A and cytoplasmic expression of nucleophosmin. Leuk Off J Leuk Soc Am Leuk Res Fund, UK. 2005;19(10):1760–7.

59. Asou H, Tashiro S, Hamamoto K, Otsuji A, Kita K, Kamada N. Establishment of a human acute myeloid leukemia cell line (Kasumi-1) with 8;21 chromosome translocation. Blood. 1991;77(9):2031–6.

60. Kozu BT, Miyoshi H, Shimizu K, Maseki N, Kaneko Y, Asou H, et al. Junctions of the AMLl/MTG8(ETO) Fusion Are Constant in t(8;21) Acute Myeloid Leukemia Detected by Reverse Transcription Polymerase Chain Reaction. 2017;8(4):1270–7.

61. 293T (ATCC® CRL-3216™) [Internet]. [cited 2017 Oct 15]. Available from: https://www.lgcstandards-atcc.org/products/all/CRL-3216.aspx?geo_country=pt#documentation

62. Perner F, Schnöder TM, Fischer T, Heidel FH. Kinomics Screening Identifies Aberrant Phosphorylation of CDC25C in FLT3-ITD-positive AML. Anticancer Res [Internet]. 2016;36(12):6249–58. Available from: http://ar.iiarjournals.org/content/36/12/6249.abstract

63. Andersson a, Edén P, Lindgren D, Nilsson J, Lassen C, Heldrup J, et al. Gene expression profiling of leukemic cell lines reveals conserved molecular signatures among subtypes with specific genetic aberrations. Leukemia [Internet]. 2005;19(6):1042–50. Available from: http://www.ncbi.nlm.nih.gov/pubmed/15843827

64. MAT2A methionine adenosyltransferase 2A [Homo sapiens (human)] [Internet]. [cited 2017 Oct 12]. Available from: https://www.ncbi.nlm.nih.gov/gene/4144

65. NIH - National Cancer Institute: Cancer Stat Facts: Acute Myeloid Leukemia (AML) [Internet]. [cited 2017 Oct 26]. Available from: https://seer.cancer.gov/statfacts/html/amyl.html

66. Beroukhim R, Mermel CH, Porter D, Wei G, Raychaudhuri S, Donovan J, et al. The landscape of somatic copy-number alteration across human cancers. Nature [Internet]. 2010;463(7283):899–905. Available from: http://www.nature.com/doifinder/10.1038/nature08822

67. Zhang W, Sviripa V, Chen X, Shi J, Yu T, Hamza A. Fluorinated N,N-

dialkylaminostilbenes repress colon cancer by targeting methionine S-adenosyltransferase 2A. 2014;8(4):796–803.

7. Annexes

7.1. QIAprep ® Spin Miniprep Kit

Quick-Start Protocol

QIAprep® Spin Miniprep Kit

The QIAprep Spin Miniprep Kit (cat. nos. 27104 and 27106) can be stored at room temperature (15–25°C) for up to 12 months.

For more information, please refer to the *QIAprep Miniprep Handbook, December 2006*, which can be found at: www.qiagen.com/handbooks.

For technical assistance, please call toll-free 00800-22-44-6000, or find regional phone numbers at www.qiagen.com/contact.

Notes before starting

- **Optional**: Add LyseBlue reagent to Buffer P1 at a ratio of 1 to 1000.
- Add the provided RNase A solution to Buffer P1, mix, and store at 2–8°C.
- Add ethanol (96–100%) to Buffer PE before use (see bottle label for volume).
- All centrifugation steps are carried out at 13,000 rpm (~17,900 x *g*) in a conventional table-top microcentrifuge.

1. Pellet 1–5 ml bacterial overnight culture by centrifugation at >8000 rpm (6800 x *g*) for 3 min at room temperature (15–25°C).
2. Resuspend pelleted bacterial cells in 250 µl Buffer P1 and transfer to a microcentrifuge tube.
3. Add 250 µl Buffer P2 and mix thoroughly by inverting the tube 4–6 times until the solution becomes clear. Do not allow the lysis reaction to proceed for more than 5 min. If using LyseBlue reagent, the solution will turn blue.
4. Add 350 µl Buffer N3 and mix immediately and thoroughly by inverting the tube 4–6 times. If using LyseBlue reagent, the solution will turn colorless.
5. Centrifuge for 10 min at 13,000 rpm (~17,900 x *g*) in a table-top microcentrifuge.

October 2010

QIAGEN®

Sample & Assay Technologies

6. Apply the supernatant from step 5 to the QIAprep spin column by decanting or pipetting. ▲ Centrifuge for 30–60 s and discard the flow-through, or ● apply vacuum to the manifold to draw the solution through the QIAprep spin column and switch off the vacuum source.
7. Recommended: Wash the QIAprep spin column by adding 0.5 ml Buffer PB. ▲ Centrifuge for 30–60 s and discard the flow-through, or ● apply vacuum to the manifold to draw the solution through the QIAprep spin column and switch off the vacuum source.

   Note: This step is only required when using *endA*$^+$ strains or other bacteria strains with high nuclease activity or carbohydrate content.
8. Wash the QIAprep spin column by adding 0.75 ml Buffer PE. ▲ Centrifuge for 30–60 s and discard the flow-through, or ● apply vacuum to the manifold to draw the solution through the QIAprep spin column and switch off the vacuum source. Transfer the QIAprep spin column to the collection tube.
9. Centrifuge for 1 min to remove residual wash buffer.
10. Place the QIAprep column in a clean 1.5 ml microcentrifuge tube. To elute DNA, add 50 µl Buffer EB (10 mM Tris·Cl, pH 8.5) or water to the center of the QIAprep spin column, let stand for 1 min, and centrifuge for 1 min.

For up-to-date licensing information and product-specific disclaimers, see the respective QIAGEN kit handbook or user manual.

Trademarks: QIAGEN®, QIAprep® (QIAGEN Group). 1063640 10/2010
© 2010 QIAGEN, all rights reserved.

7.2. QIAquick ® Gel Extraction Kit

Quick-Start Protocol July 2015

QIAquick® Gel Extraction Kit

The QIAquick Gel Extraction Kit (cat. nos. 28704 and 28706) can be stored at room temperature (15–25°C) for up to 12 month.

Further information

- *QIAquick Spin Handbook*: **www.qiagen.com/HB-1196**
- Safety Data Sheets: **www.qiagen.com/safety**
- Technical assistance: **support.qiagen.com**

Notes before starting

- This protocol is for the purification of up to 10 µg DNA (70 bp to 10 kb).
- The yellow color of Buffer QG indicates a pH ≤7.5. DNA adsorption to the membrane is only efficient at pH ≤7.5.
- Add ethanol (96–100%) to Buffer PE before use (see bottle label for volume).
- Isopropanol (100%) and a heating block or water bath at 50°C are required.
- All centrifugation steps are carried out at 17,900 *x g* (13,000 rpm) in a conventional table-top microcentrifuge.

1. Excise the DNA fragment from the agarose gel with a clean, sharp scalpel.
2. Weigh the gel slice in a colorless tube. Add 3 volumes Buffer QG to 1 volume gel (100 mg gel ~ 100 µl). The maximum amount of gel per spin column is 400 mg. For >2% agarose gels, add 6 volumes Buffer QG.
3. Incubate at 50°C for 10 min (or until the gel slice has completely dissolved). Vortex the tube every 2–3 min to help dissolve gel. After the gel slice has dissolved completely, check that the color of the mixture is yellow (similar to Buffer QG without dissolved agarose). If the color of the mixture is orange or violet, add 10 µl 3 M sodium acetate, pH 5.0, and mix. The mixture turns yellow.

Sample to Insight

4. Add 1 gel volume isopropanol to the sample and mix.
5. Place a QIAquick spin column in a provided 2 ml collection tube or into a vacuum manifold. To bind DNA, apply the sample to the QIAquick column and centrifuge for 1 min or apply vacuum to the manifold until all the samples have passed through the column. Discard flow-through and place the QIAquick column back into the same tube. For sample volumes of >800 µl, load and spin/apply vacuum again.
6. If DNA will subsequently be used for sequencing, in vitro transcription, or microinjection, add 500 µl Buffer QG to the QIAquick column and centrifuge for 1 min or apply vacuum. Discard flow-through and place the QIAquick column back into the same tube.
7. To wash, add 750 µl Buffer PE to QIAquick column and centrifuge for 1 min or apply vacuum. Discard flow-through and place the QIAquick column back into the same tube.

   Note: If the DNA will be used for salt-sensitive applications (e.g., sequencing, blunt-ended ligation), let the column stand 2–5 min after addition of Buffer PE.

   Centrifuge the QIAquick column in the provided 2 ml collection tube for 1 min to remove residual wash buffer.

8. Place QIAquick column into a clean 1.5 ml microcentrifuge tube.
9. To elute DNA, add 50 µl Buffer EB (10 mM Tris·Cl, pH 8.5) or water to the center of the QIAquick membrane and centrifuge the column for 1 min. For increased DNA concentration, add 30 µl Buffer EB to the center of the QIAquick membrane, let the column stand for 1 min, and then centrifuge for 1 min. After the addition of Buffer EB to the QIAquick membrane, increasing the incubation time to up to 4 min can increase the yield of purified DNA.
10. If purified DNA is to be analyzed on a gel, add 1 volume of Loading Dye to 5 volumes of purified DNA. Mix the solution by pipetting up and down before loading the gel.

Scan QR code for handbook.

For up-to-date licensing information and product-specific disclaimers, see the respective QIAGEN kit handbook or user manual. Trademarks: QIAGEN®, Sample to Insight®, QIAquick® (QIAGEN Group). 1095985 07/2015 HB-0901-002 © 2015 QIAGEN, all rights reserved.

7.3. PureLink® HiPure Plasmid Filter DNA Purification Kits

QUICK REFERENCE

invitrogen by life technologies

PureLink® HiPure Plasmid Filter DNA Purification Kits

Catalog numbers K2100-14, K2100-15, K2100-16, K2100-17, K2100-26, K2100-27

Publication Part Number 7015018 MAN0003720 **Revision Date** 2 May 2011

Before starting

- Add RNase A to Resuspension Buffer (R3) according to the instructions on the label.
- Warm Lysis Buffer (L7) briefly at 37°C to redissolve any particulate matter, if necessary.

Midiprep Procedure

Notes

- For all column steps, use Column Holders (included) or a Nucleic Acid Purification Rack.
- Grow transformed *E. coli* in LB medium. Use 15–25 mL (high copy number plasmid) or 25–100 mL (low copy number plasmid) of an overnight culture.

Isolate midiprep plasmid DNA

1. **Equilibrate.** Apply 15 mL Equilibration Buffer (EQ1) directly into the Filtration Cartridge, which is inserted in the PureLink® HiPure Midi Column. Allow the solution in the column to drain by gravity flow.
2. **Harvest.** Centrifuge the overnight LB culture at 4000 × g for 10 minutes in a 50-mL disposable centrifuge tube. Remove all medium.
3. **Resuspend.** Add 10 mL Resuspension Buffer (R3) with RNase A to the cell pellet and gently shake the pellet until the cell suspension is homogenous.
4. **Lyse**. Add 10 mL Lysis Buffer (L7). Mix gently by inverting the capped tube until the mixture is homogeneous. Do not vortex. Incubate the tube at room temperature for 5 minutes.
5. **Precipitate.** Add 10 mL Precipitation Buffer (N3). Mix by inverting the tube until the mixture is homogeneous.
6. **Clarify.** Transfer the precipitated lysate into the column. Allow the lysate to drain by gravity flow. *Optional:* Wash the column with 10 mL Wash Buffer (W8). Allow the buffer to flow through the column by gravity flow.
7. **Wash.** Discard the inner filtration cartridge. Add 20 mL Wash Buffer (W8) to the column. Discard the flow-through after Wash Buffer (W8) drains from the column.
8. **Elute.** Place a sterile 15-mL centrifuge tube under the column. Add 5 mL Elution Buffer (E4) to the column. Allow the solution to drain by gravity flow. Discard the column. *The elution tube contains the purified DNA.* Proceed to **Precipitate DNA.**

Intended Use

For research use only. Not intended for any animal or human therapeutic or diagnostic use.

life technologies

Midiprep Procedure, Continued

Precipitate DNA

1. **Precipitate.** Add 3.5 mL isopropanol to the eluate. Incubate DNA with isopropanol for 2 minutes at room temperature. Centrifuge the tube at >12,000 × g for 30 minutes at 4°C.
2. **Wash.** Discard the supernatant. Add 3 mL 70% ethanol to the pellet. Centrifuge the tube at >12,000 × g for 5 minutes at 4°C. Remove the supernatant.
3. **Resuspend.** Air-dry the pellet for 10 minutes. Resuspend the purified DNA in 100–200 µL TE Buffer (TE). Store plasmid DNA at –20°C.

Maxiprep Procedure

Notes

- For all column steps, use Column Holders (included) or a Nucleic Acid Purification Rack.
- Grow transformed *E. coli* in LB medium. Use 100–200 mL (high copy number plasmid) or 250–500 mL (low copy number plasmid) of an overnight culture.

Isolate maxiprep plasmid DNA

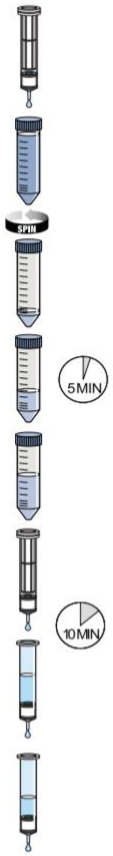

1. **Equilibrate.** Apply 30 mL Equilibration Buffer (EQ1) directly into the Filtration Cartridge, which is inserted in the PureLink® HiPure Maxi Column. Allow the solution in the column to drain by gravity flow.
2. **Harvest.** Centrifuge the overnight LB culture at 4000 × g for 10 minutes. Remove medium.
3. **Resuspend.** Add 10 mL Resuspension Buffer (R3) with RNase A to the cell pellet and gently shake the pellet until the cell suspension is homogenous.
4. **Lyse**. Add 10 mL Lysis Buffer (L7). Mix gently by inverting the capped tube until the mixture is homogeneous. Do not vortex. Incubate the tube at room temperature for 5 minutes.
5. **Precipitate.** Add 10 mL Precipitation Buffer (N3). Mix immediately by inverting the tube until the mixture is homogeneous. Do not vortex.
6. **Clarify.** Transfer the precipitated lysate into the column. Allow the lysate to filter through the column by gravity flow. *Optional:* Wash the column with 10 mL Wash Buffer (W8). Allow the buffer to flow through the column by gravity flow.
7. **Wash.** Discard the inner filtration cartridge. Wash the column with 50 mL Wash Buffer (W8). Discard the flow-through after the buffer drains.
8. **Elute.** Place a sterile 50-mL centrifuge tube under the HiPure Filter Column. Add 15 mL Elution Buffer (E4) to the column. Allow the solution to drain by gravity flow. Discard the column. *The elution tube contains the purified DNA.*

   Proceed to **Precipitate DNA using a Centrifuge** (for Cat. nos. K2100-16 and K2100-17) or **Precipitate DNA with a PureLink® HiPure Precipitator Module** (for Cat. nos. K2100-26 and K2100-27).

Troubleshooting

Problem	Solution
Low plasmid DNA yield	• Store Lysis Buffer (L7) and Equilibration Buffer (EQ1) at room temperature. Store Resuspension Buffer (R3) with RNase A at 4°C. • Increase the volume of starting material. Doubling the volumes of Resuspension Buffer (R3), Lysis Buffer (L7) and Precipitation Buffer (N3) may increase plasmid yield and quality. • Attach the precipitator to the syringe nozzle using the luer lock mechanism without applying excessive force. Before removing the plunger from the syringe, always remove the precipitator to avoid damaging the membrane. Do not apply excessive pressure while pushing the solution through the precipitator.
Contaminating Genomic DNA	Gently invert tubes to mix after adding Buffers L7 and N3, respectively. Do not vortex.
Precipitator is clogged (FP Maxiprep Kit)	• Load the eluate from **one** anion exchange column onto the precipitator. • Ethanol-precipitated DNA consists of fine particles that may clog the precipitator. Always use isopropanol to precipitate plasmid DNA.
Plasmid DNA is degraded	Incubate the lysate, after the addition of Lysis Buffer (L7), at room temperature for no longer than 5 minutes.
Contaminating RNA	• Make sure that RNase A is added to Resuspension Buffer (R3). If necessary, increase RNase A concentration to 400 µg/mL. • Carefully remove all media before resuspending cells. • Perform column washing and elution steps without any delays. • Wash droplets of lysate from the column wall with Wash Buffer (W8).
Bacterial lysate is slowly filtered with columns	• Reduce volume of culture used. • Remove precipitated cell debris from overgrown cultures by centrifuging the bacterial lysate at 12,000 × g for 5 minutes.
Enzymatic reactions are inhibited	Remove ethanol by air-drying as described in the protocol.

Limited Use Label License: Research Use Only

The purchase of this product conveys to the purchaser the limited, non-transferable right to use the purchased amount of the product only to perform internal research for the sole benefit of the purchaser. No right to resell this product or any of its components is conveyed expressly, by implication, or by estoppel. This product is for internal research purposes only and is not for use in commercial applications of any kind, including, without limitation, quality control and commercial services such as reporting the results of purchaser's activities for a fee or other form of consideration. For information on obtaining additional rights, please contact outlicensing@lifetech.com or Out Licensing, Life Technologies, 5791 Van Allen Way, Carlsbad, California 92008.

©2011 Life Technologies Corporation. All rights reserved. The trademarks mentioned herein are the property of Life Technologies Corporation or their respective owners.

Headquarters
5791 Van Allen Way | Carlsbad, CA 92008 USA
Phone +1 760 603 7200 | Toll Free in USA 800 955 6288
For support visit www.invitrogen.com/support or email techsupport@invitrogen.com
www.lifetechnologies.com